Supplementary Information for:

Rates of Antarctic Ice Sheet thinning since Last Glacial Maximum rival future projections

Roger Creel[1,*]
Ryan Venturelli[2]
Anna Ruth Halberstadt[3]
Sam Chester[4]
Ava Nordgren[3]
John Schiavo[4]

[1]Department of Geology and Geophysics, Texas A&M University, 3115 TAMU, College Station, Texas, 77843, USA.
[2]Department of Geology and Geological Engineering, Colorado School of Mines, Berthoud Hall 411E, Golden, Colorado, 80401, USA.
[3]Department of Earth & Planetary Sciences, Jackson School of Earth Sciences, University of Texas at Austin, 2305 Speedway Suite 2.112, Austin, Texas, 78712, USA.
[4]Lamont-Doherty Earth Observatory, Columbia University of New York, 61 Route 9W, Palisades, 10964, New York, USA.

***Corresponding author**
E-mail: roger.creel@tamu.edu

Supplementary Overview

This Supplement contains 4 subsections, which provide extended analyses and supporting figures. The sections are organized as follows:

1. **Site-by-site comparisons of past, present, and future thinning rates**
2. **Skytrain Ice Rise thinning profile**
3. **PATR sensitivity to modeling choices**
4. **Site-by-site comparison of PATR to data**

1 Site-by-site comparisons of past, present, and future thinning rates

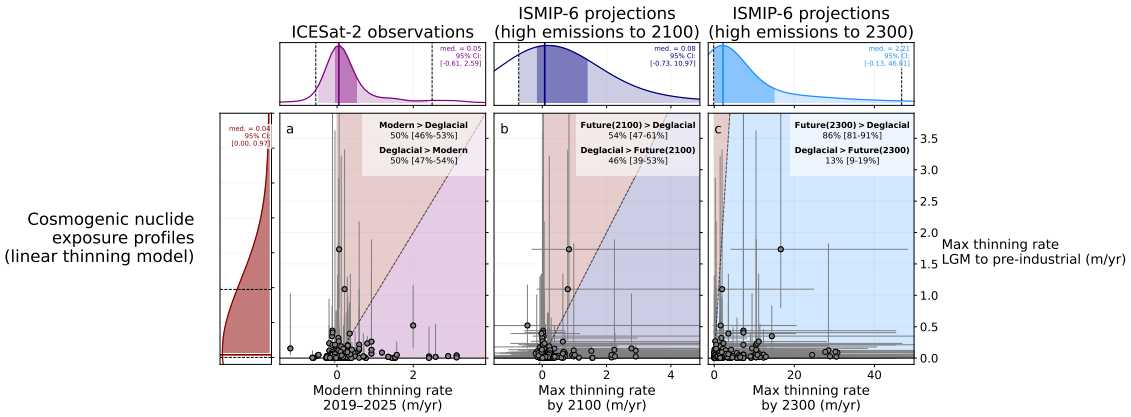

Fig. S1 Site-by-site comparison of past to modern and future local decadal ice thinning rates. As in Figure **??**, but modern and future rates are compared to cosmogenic nuclide exposure profiles fit with probabilistic linear orthogonal distance regression models. See Figure **??** caption and Methods for more details.

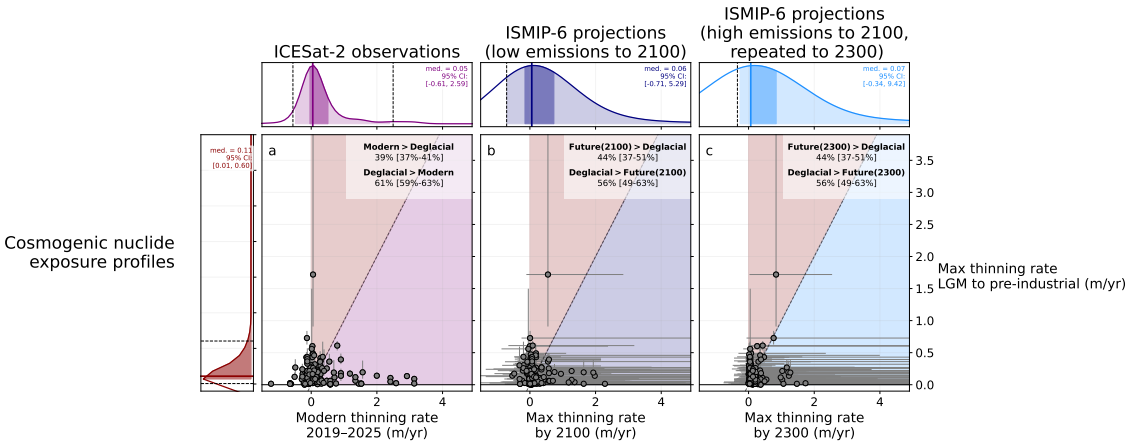

Fig. S2 Additional comparison of past to modern and future ice thinning rates. As in Figure **??**, but (b) depicts ISMIP-6 projections to 2100 under a low emissions scenario (SSP1-2.6) and (c) shows ISMIP-6 projections to 2300 with high emissions forcing (RCP8.5 / SSP5-8.5) to 2100, then 2100 forcing repeated to 2300 [1]. See Figure **??** caption for more details.

2 Skytrain Ice Rise thinning profile

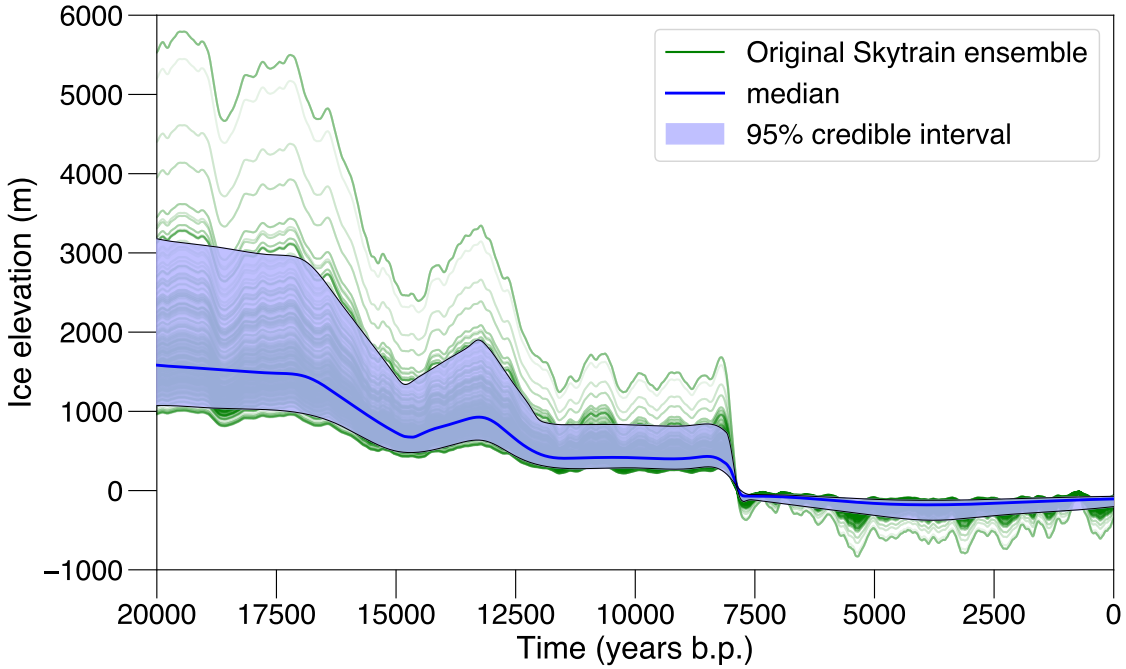

Fig. S3 Postglacial ice thinning rates from the Skytrain Ice Rise. Green lines indicate ice elevations derived from oxygen isotope measurements in the Skytrain Ice Rise [2]. Blue envelope marks median and 95% credible interval computed using segmented linear regression.

3 PATR sensitivity to modeling choices

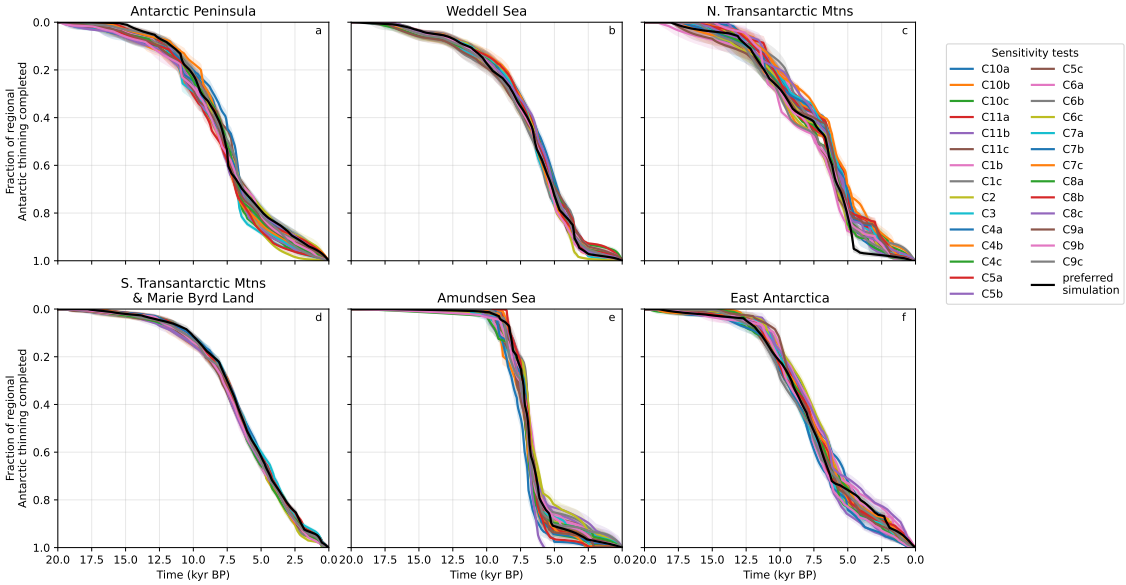

Fig. S4 Tests demonstrating sensitivity of PATR to model parameters. Colored lines and envelopes indicate fractional Antarctic Ice Sheet thinning completed for sensitivity tests for each Antarctic region (see Methods); black line marks preferred PATR reconstruction.

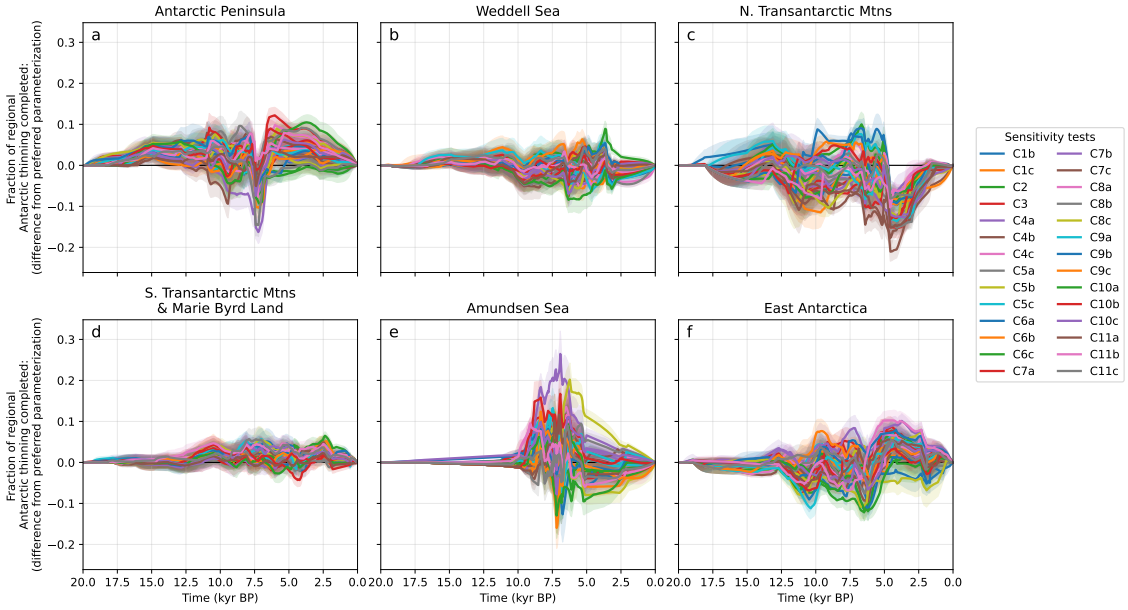

Fig. S5 Tests demonstrating sensitivity of PATR to model parameters. Colored lines and envelopes indicate difference in fractional Antarctic Ice Sheet thinning completed for each Antarctic region between the preferred parameterization and all sensitivity tests (see Methods).

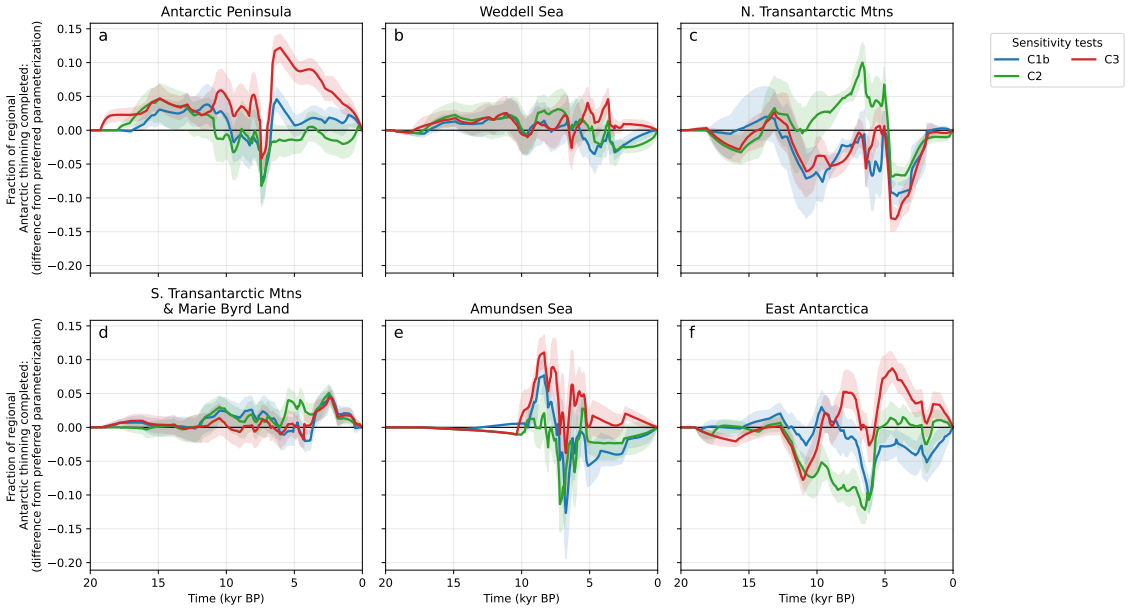

Fig. S6 Tests demonstrating sensitivity of PATR to model parameters. Colored lines and envelopes indicate difference in fractional Antarctic Ice Sheet thinning completed for each Antarctic region between the preferred parameterization and sensitivity tests C1a, C1b, C1c, C2, and C3 (see Methods).

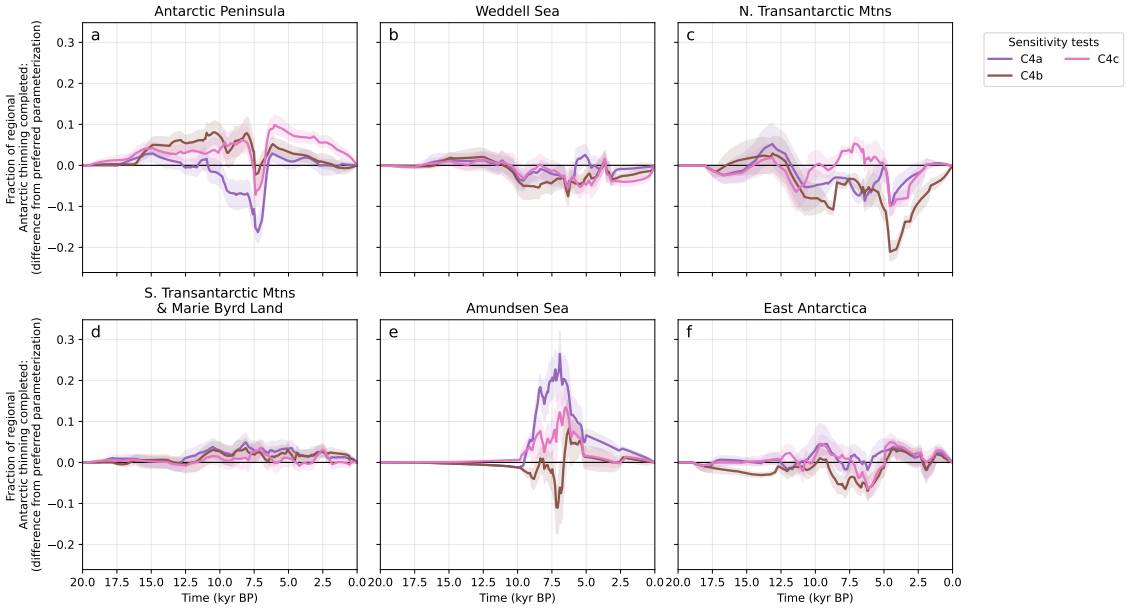

Fig. S7 Tests demonstrating sensitivity of PATR to model parameters. Colored lines and envelopes indicate difference in fractional Antarctic Ice Sheet thinning completed for each Antarctic region between the preferred parameterization and sensitivity tests C4a, C4b, and C4c (see Methods).

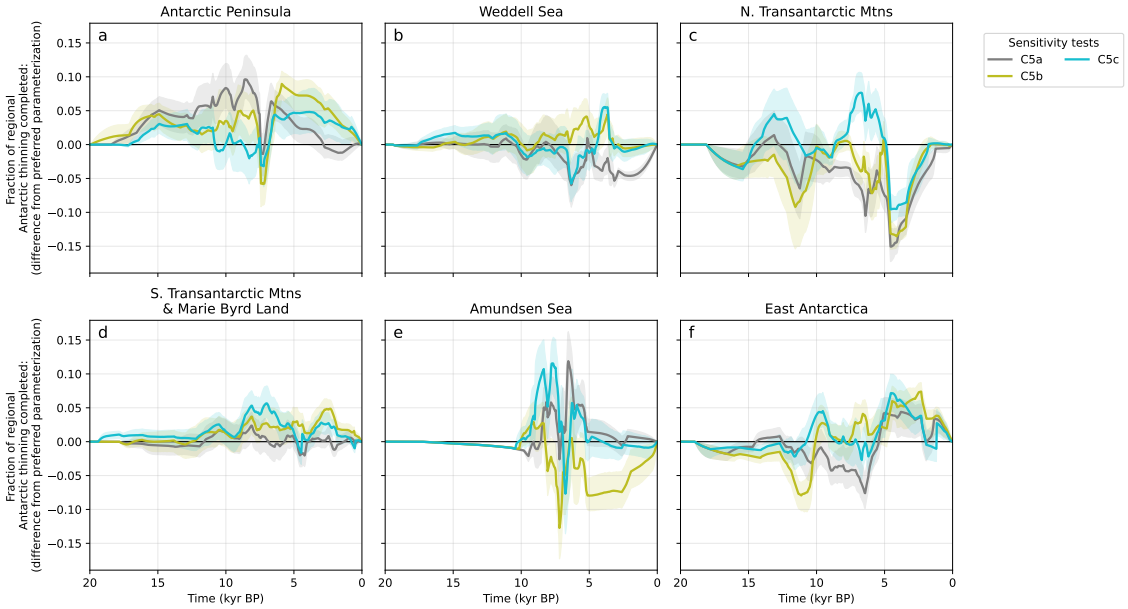

Fig. S8 Tests demonstrating sensitivity of PATR to model parameters. Colored lines and envelopes indicate difference in fractional Antarctic Ice Sheet thinning completed for each Antarctic region between the preferred parameterization and sensitivity tests C5a, C5b, and C5c (see Methods).

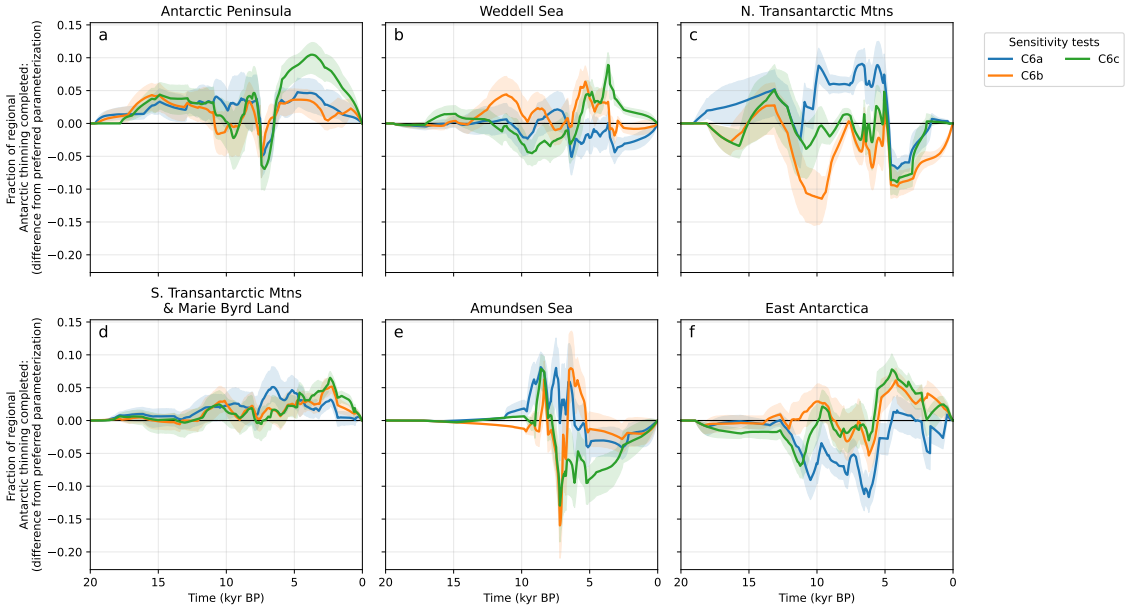

Fig. S9 Tests demonstrating sensitivity of PATR to model parameters. Colored lines and envelopes indicate difference in fractional Antarctic Ice Sheet thinning completed for each Antarctic region between the preferred parameterization and sensitivity tests C6a, C6b, and C6c (see Methods).

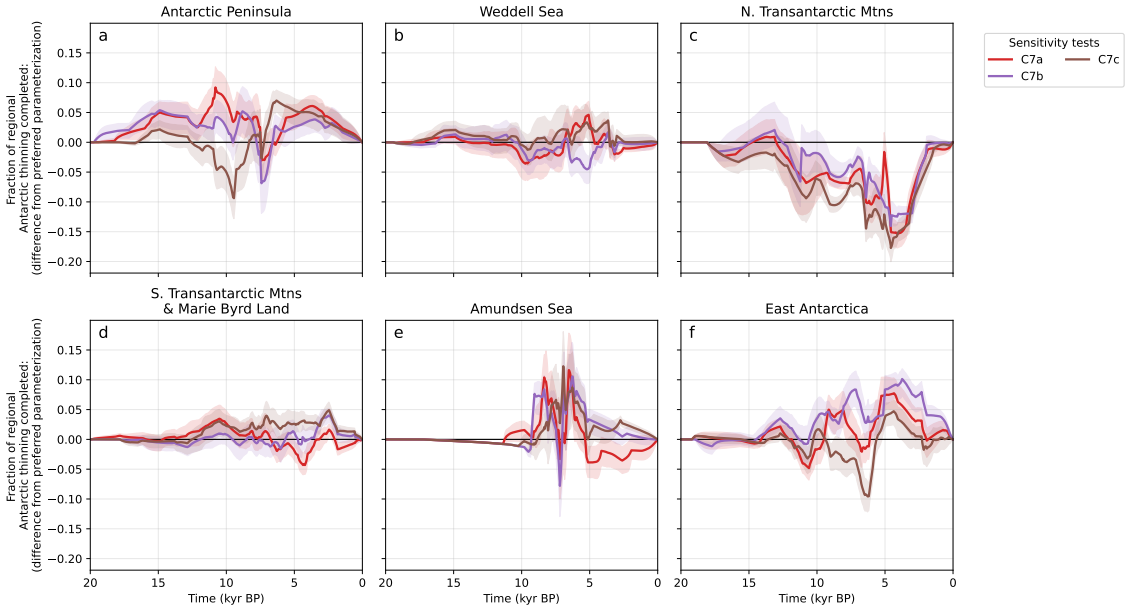

Fig. S10 Tests demonstrating sensitivity of PATR to model parameters. Colored lines and envelopes indicate difference in fractional Antarctic Ice Sheet thinning completed for each Antarctic region between the preferred parameterization and sensitivity tests C7a, C7b, and C7c (see Methods).

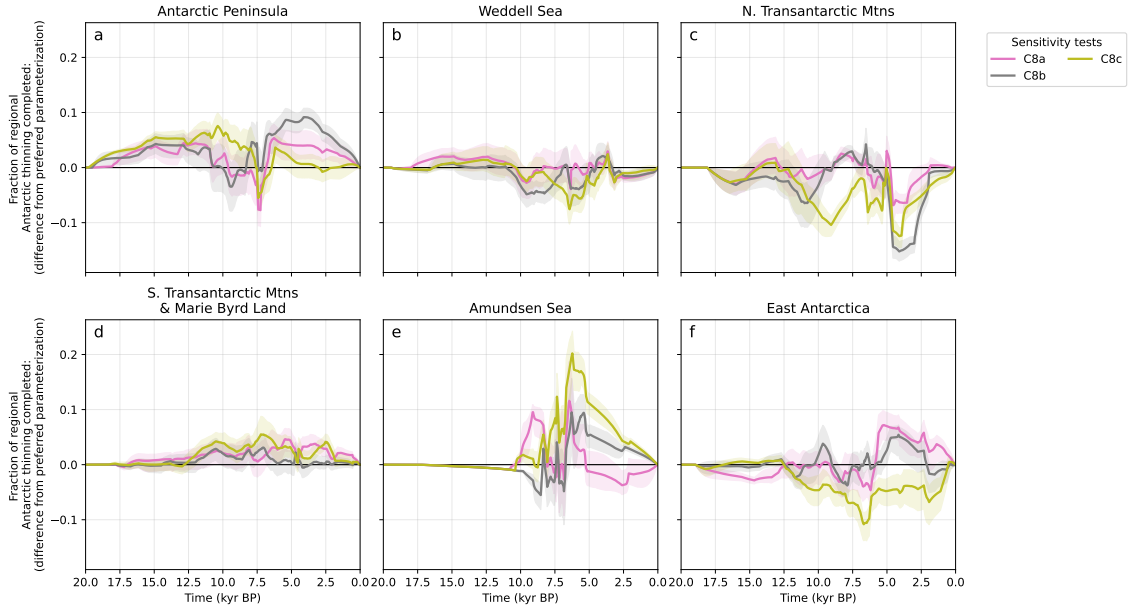

Fig. S11 Tests demonstrating sensitivity of PATR to model parameters. Colored lines and envelopes indicate difference in fractional Antarctic Ice Sheet thinning completed for each Antarctic region between the preferred parameterization and sensitivity tests C8a, C8b, and C8c (see Methods).

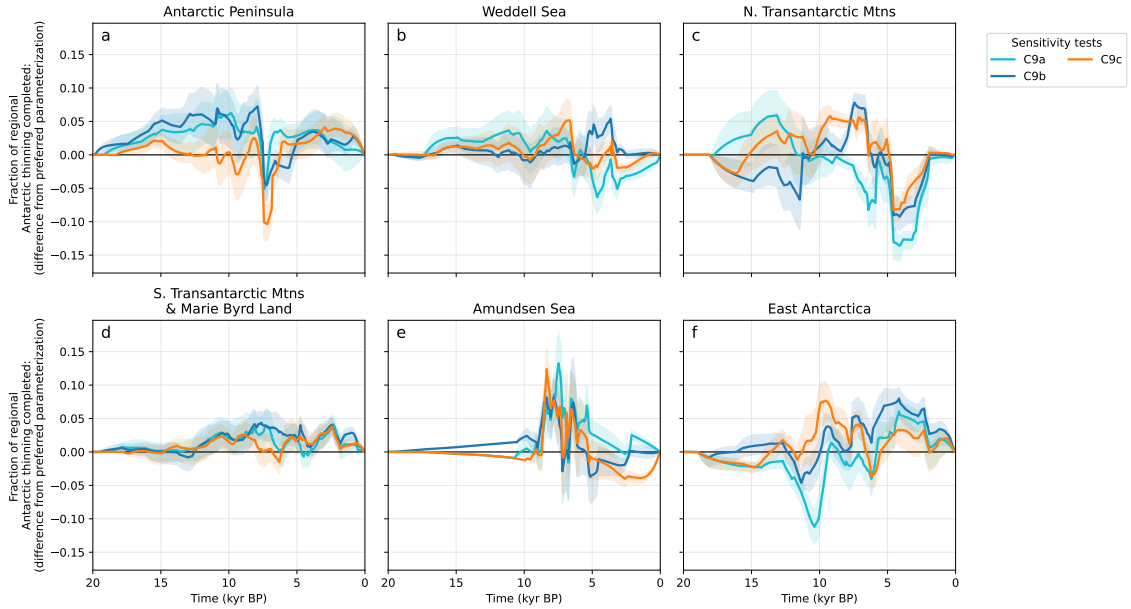

Fig. S12 Tests demonstrating sensitivity of PATR to model parameters. Colored lines and envelopes indicate difference in fractional Antarctic Ice Sheet thinning completed for each Antarctic region between the preferred parameterization and sensitivity tests C9a, C9b, and C9c (see Methods).

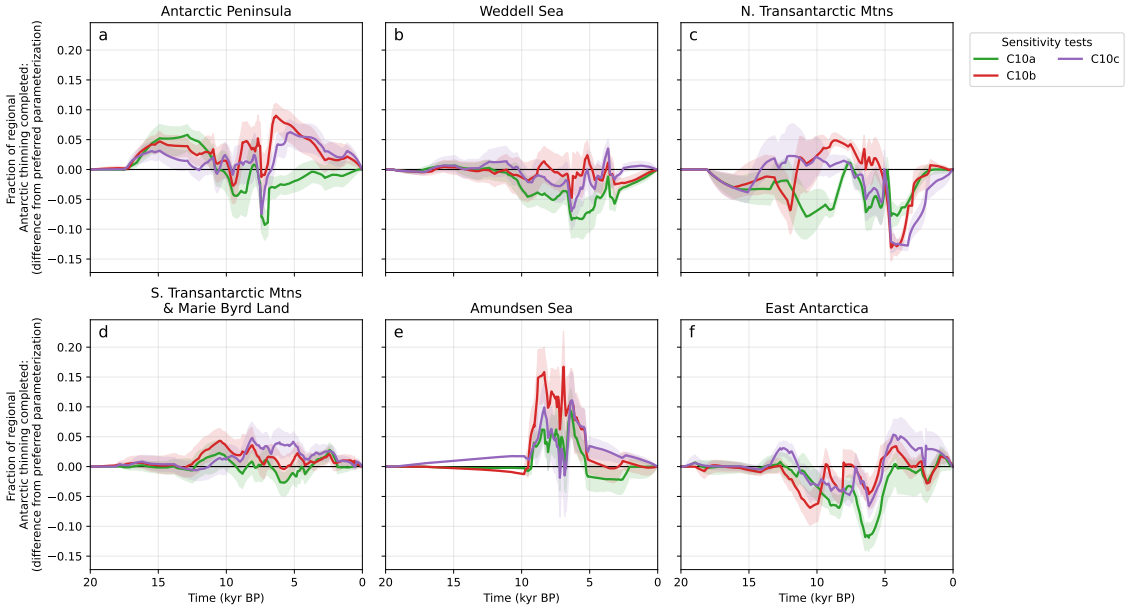

Fig. S13 Tests demonstrating sensitivity of PATR to model parameters. Colored lines and envelopes indicate difference in fractional Antarctic Ice Sheet thinning completed for each Antarctic region between the preferred parameterization and sensitivity tests C10a, C10b, and C10c (see Methods).

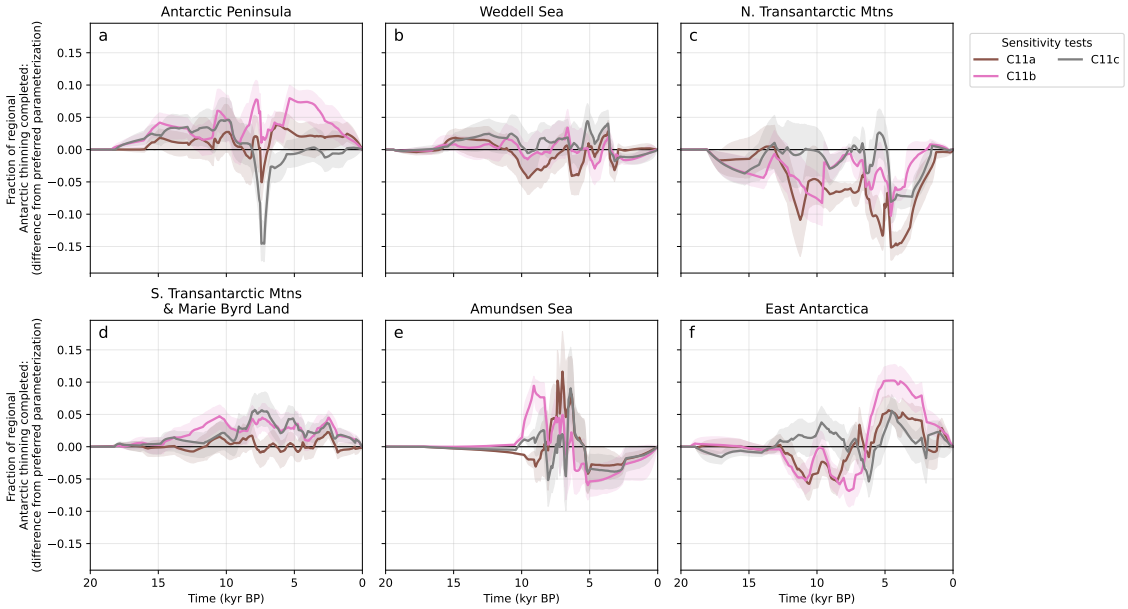

Fig. S14 Tests demonstrating sensitivity of PATR to model parameters. Colored lines and envelopes indicate difference in fractional Antarctic Ice Sheet thinning completed for each Antarctic region between the preferred parameterization and sensitivity tests C11a, C11b, and C11c (see Methods).

4 Site-by-site comparison of PATR to data

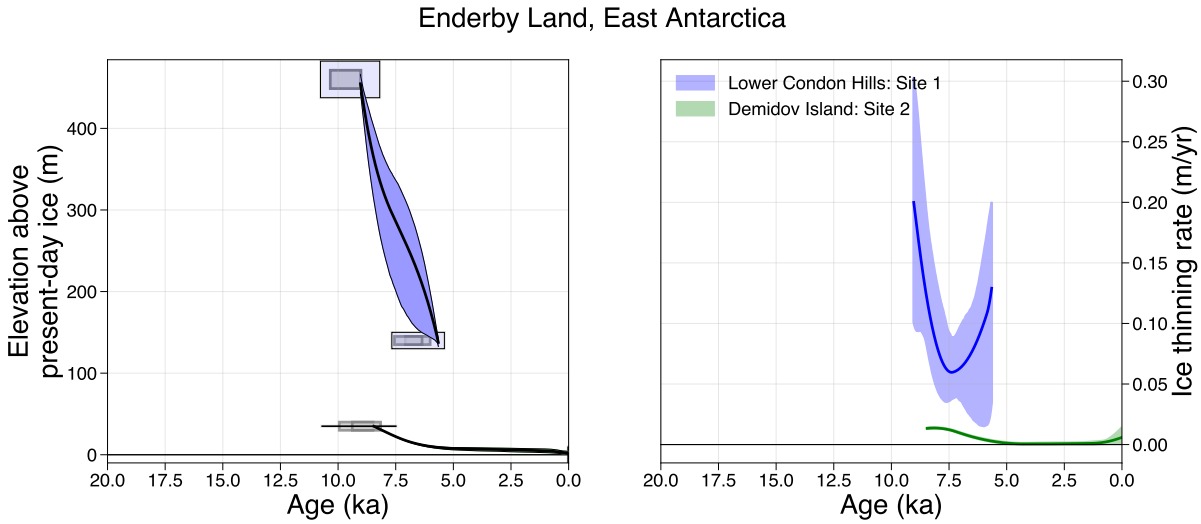

Fig. S15 Thinning histories from Enderby Land East Antarctica. Colored boxes mark cosmogenic nuclide exposure age data and/or radiocarbon-dated lakes. Gray boxes mark rejected data. Colored envelopes denote PATR median and 95% credible intervals for local Antarctic Ice Sheet elevation (left panel) and rate of thinning (right panel).

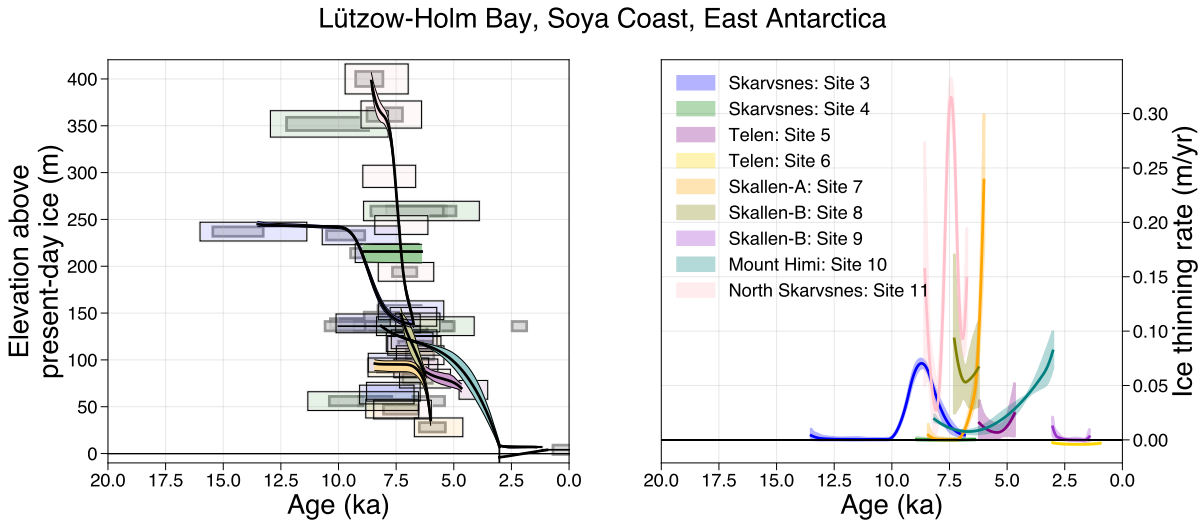

Fig. S16 Thinning histories from Lützow-Holm Bay Soya Coast East Antarctica. Colored boxes mark cosmogenic nuclide exposure age data and/or radiocarbon-dated lakes. Gray boxes mark rejected data. Colored envelopes denote PATR median and 95% credible intervals for local Antarctic Ice Sheet elevation (left panel) and rate of thinning (right panel).

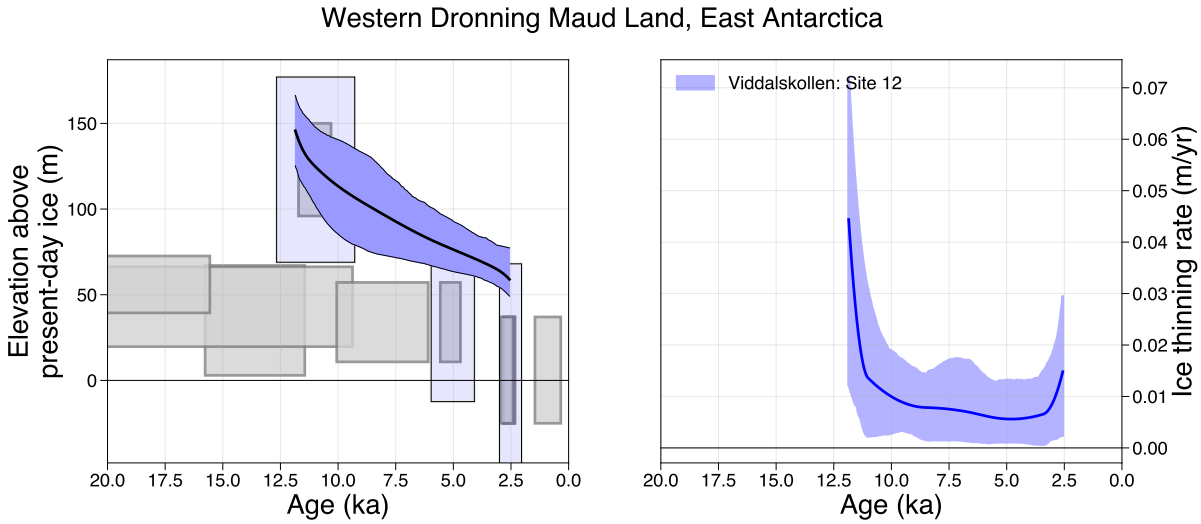

Fig. S17 Thinning histories from Western Dronning Maud Land East Antarctica. Colored boxes mark cosmogenic nuclide exposure age data and/or radiocarbon-dated lakes. Gray boxes mark rejected data. Colored envelopes denote PATR median and 95% credible intervals for local Antarctic Ice Sheet elevation (left panel) and rate of thinning (right panel).

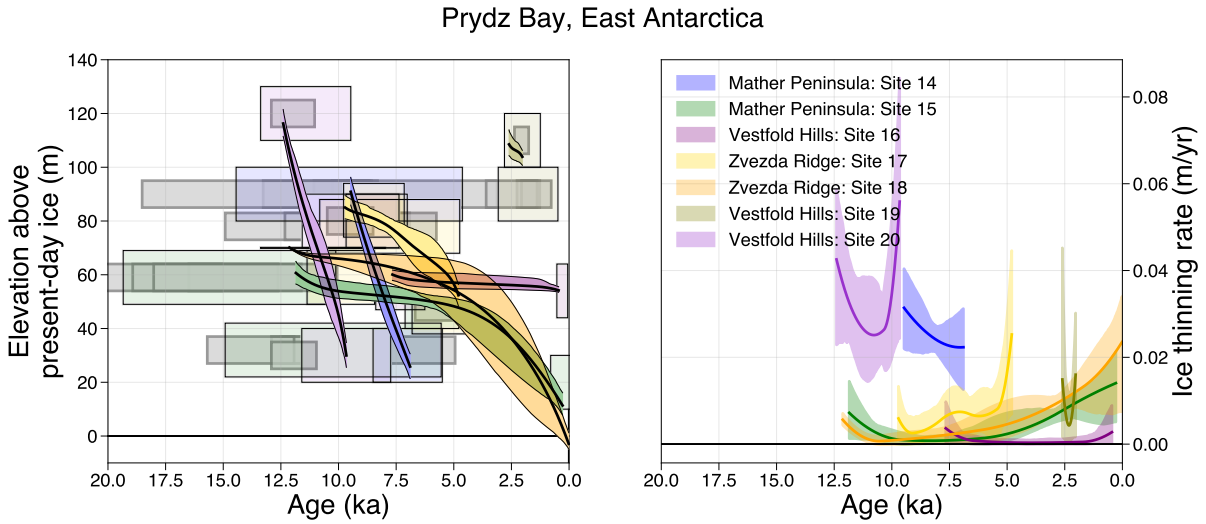

Fig. S18 Thinning histories from Prydz Bay East Antarctica. Colored boxes mark cosmogenic nuclide exposure age data and/or radiocarbon-dated lakes. Gray boxes mark rejected data. Colored envelopes denote PATR median and 95% credible intervals for local Antarctic Ice Sheet elevation (left panel) and rate of thinning (right panel).

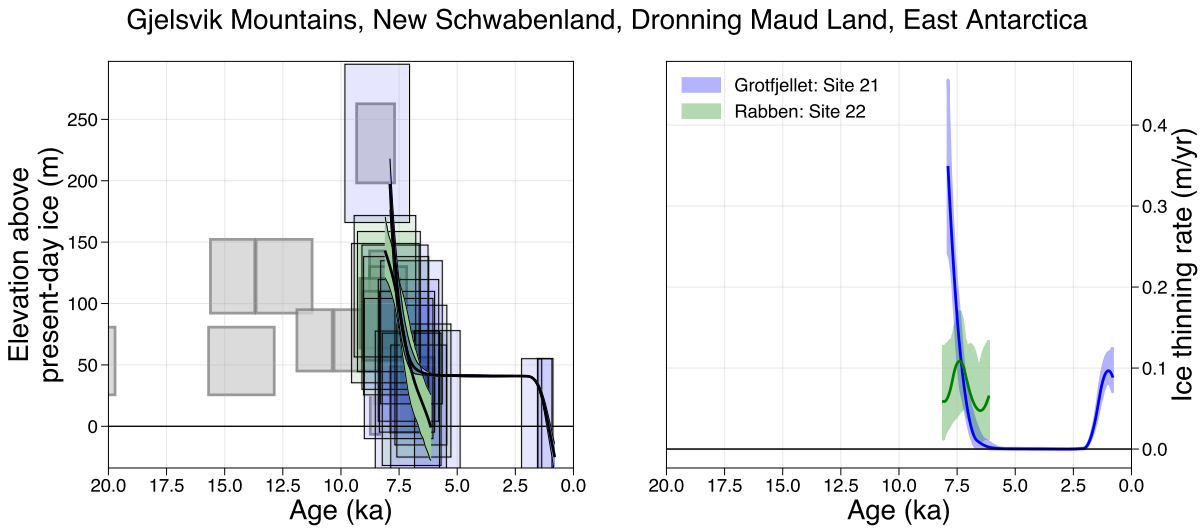

Fig. S19 Thinning histories from Gjelsvik Mountains new Schwabenland Dronning Maud Land East Antarctica. Colored boxes mark cosmogenic nuclide exposure age data and/or radiocarbon-dated lakes. Gray boxes mark rejected data. Colored envelopes denote PATR median and 95% credible intervals for local Antarctic Ice Sheet elevation (left panel) and rate of thinning (right panel).

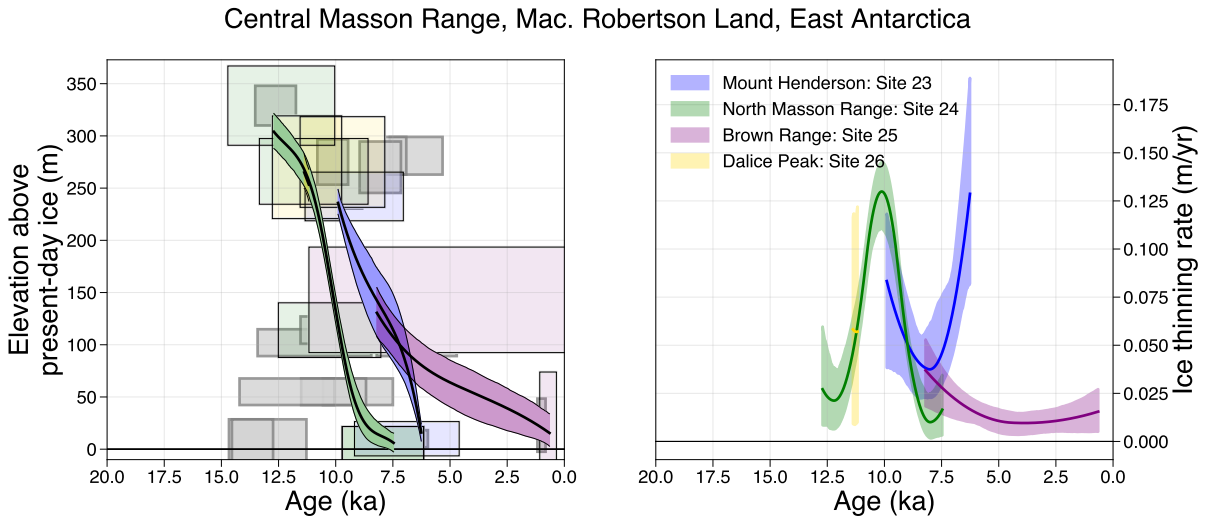

Fig. S20 Thinning histories from Central Masson Range Mac. Robertson Land East Antarctica. Colored boxes mark cosmogenic nuclide exposure age data and/or radiocarbon-dated lakes. Gray boxes mark rejected data. Colored envelopes denote PATR median and 95% credible intervals for local Antarctic Ice Sheet elevation (left panel) and rate of thinning (right panel).

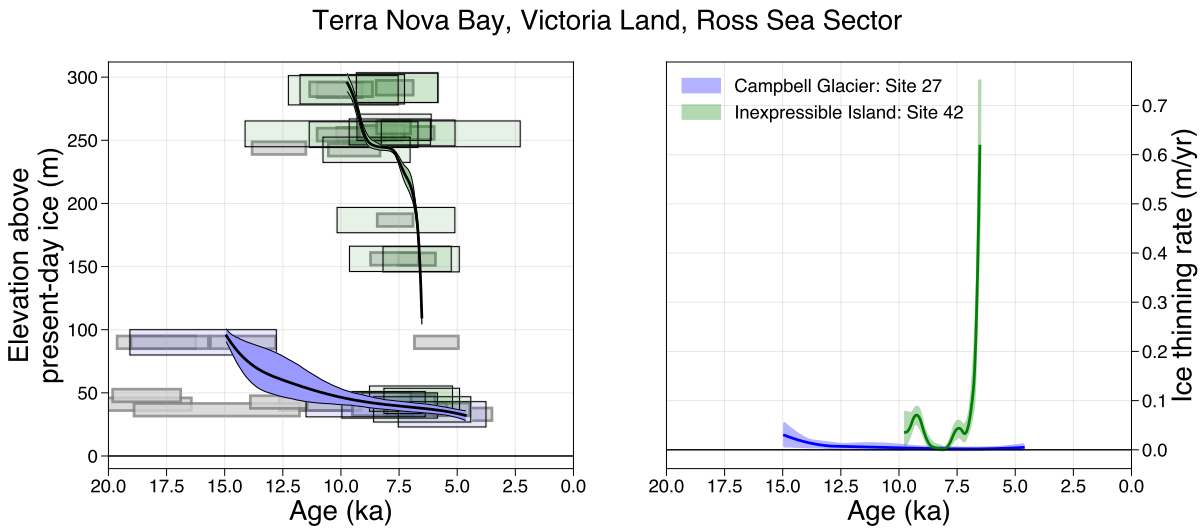

Fig. S21 Thinning histories from Terra Nova Bay Victoria Land Ross Sea Sector. Colored boxes mark cosmogenic nuclide exposure age data and/or radiocarbon-dated lakes. Gray boxes mark rejected data. Colored envelopes denote PATR median and 95% credible intervals for local Antarctic Ice Sheet elevation (left panel) and rate of thinning (right panel).

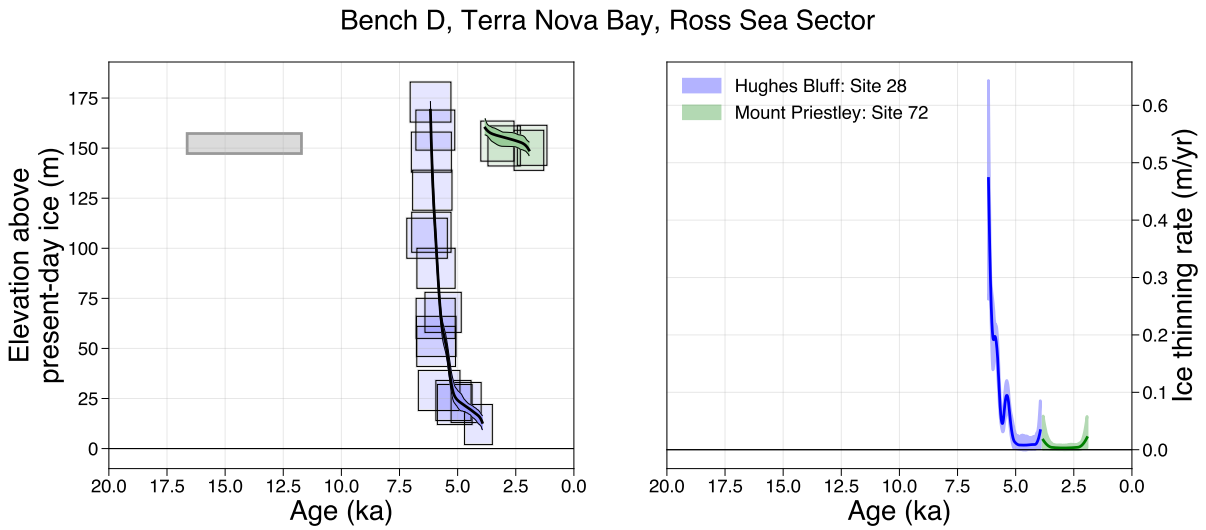

Fig. S22 Thinning histories from Bench D Terra Nova Bay Ross Sea Sector. Colored boxes mark cosmogenic nuclide exposure age data and/or radiocarbon-dated lakes. Gray boxes mark rejected data. Colored envelopes denote PATR median and 95% credible intervals for local Antarctic Ice Sheet elevation (left panel) and rate of thinning (right panel).

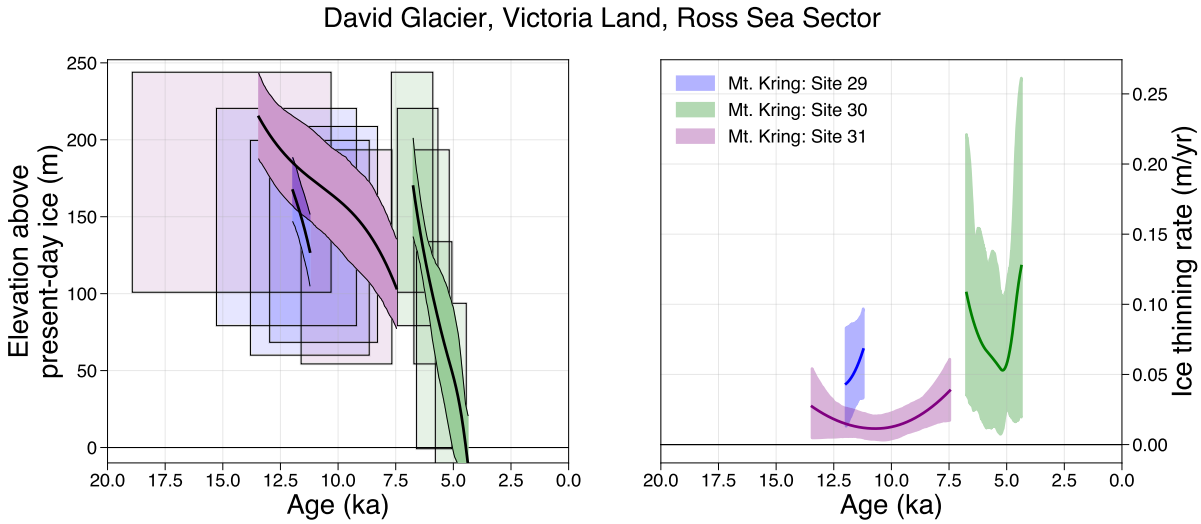

Fig. S23 Thinning histories from David Glacier Victoria Land Ross Sea Sector. Colored boxes mark cosmogenic nuclide exposure age data and/or radiocarbon-dated lakes. Gray boxes mark rejected data. Colored envelopes denote PATR median and 95% credible intervals for local Antarctic Ice Sheet elevation (left panel) and rate of thinning (right panel).

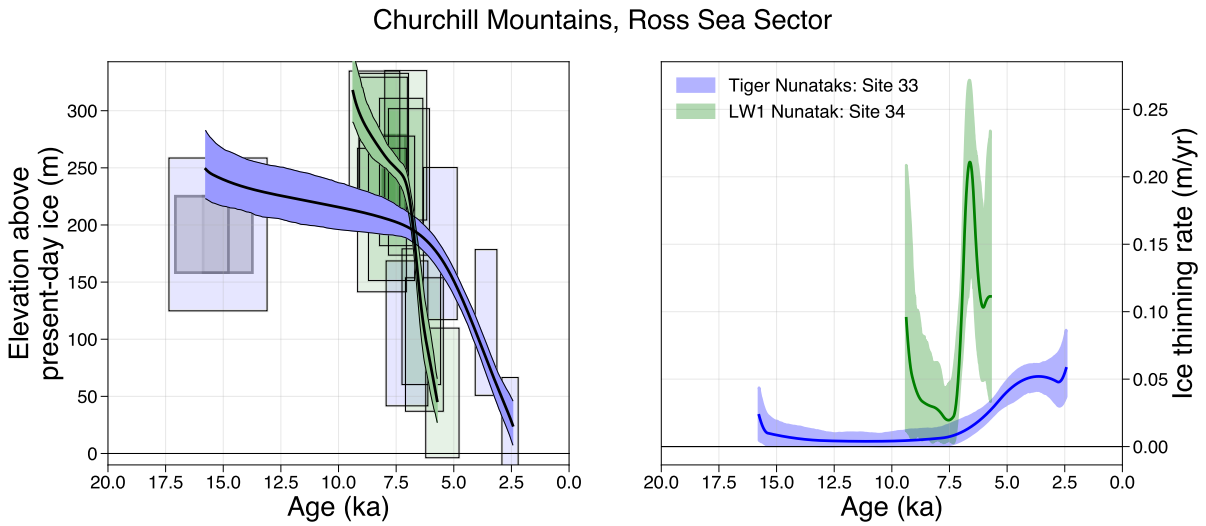

Fig. S24 Thinning histories from Churchill Mountains Ross Sea Sector. Colored boxes mark cosmogenic nuclide exposure age data and/or radiocarbon-dated lakes. Gray boxes mark rejected data. Colored envelopes denote PATR median and 95% credible intervals for local Antarctic Ice Sheet elevation (left panel) and rate of thinning (right panel).

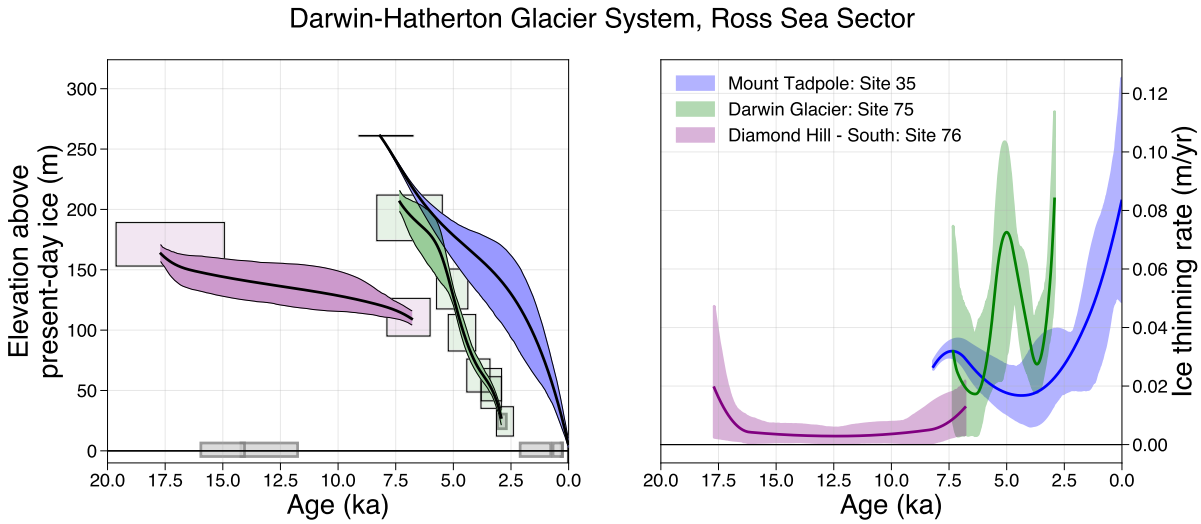

Fig. S25 Thinning histories from Darwin-Hatherton Glacier System Ross Sea Sector. Colored boxes mark cosmogenic nuclide exposure age data and/or radiocarbon-dated lakes. Gray boxes mark rejected data. Colored envelopes denote PATR median and 95% credible intervals for local Antarctic Ice Sheet elevation (left panel) and rate of thinning (right panel).

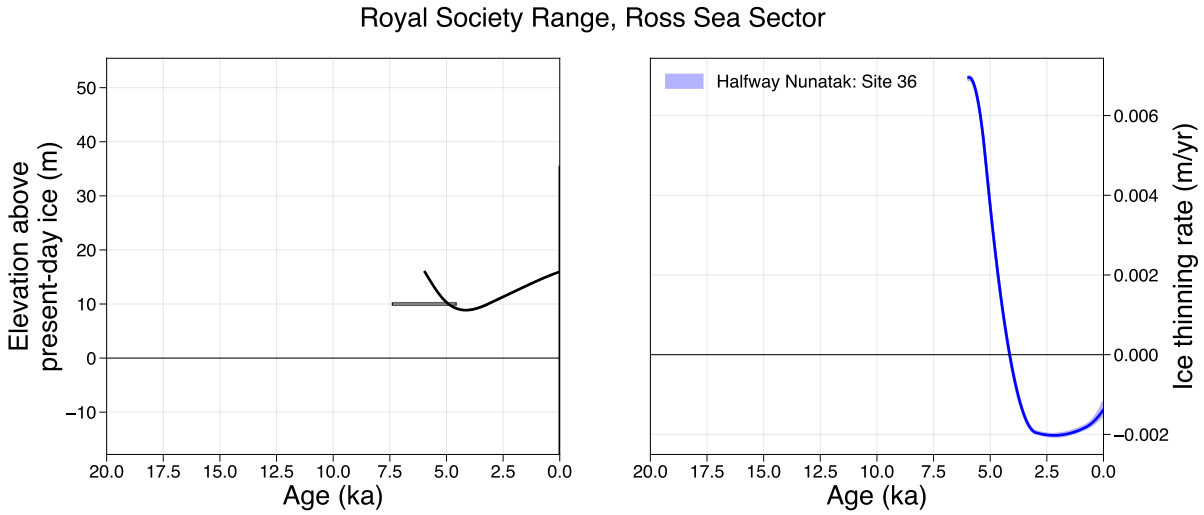

Fig. S26 Thinning histories from Royal Society Range Ross Sea Sector. Colored boxes mark cosmogenic nuclide exposure age data and/or radiocarbon-dated lakes. Gray boxes mark rejected data. Colored envelopes denote PATR median and 95% credible intervals for local Antarctic Ice Sheet elevation (left panel) and rate of thinning (right panel).

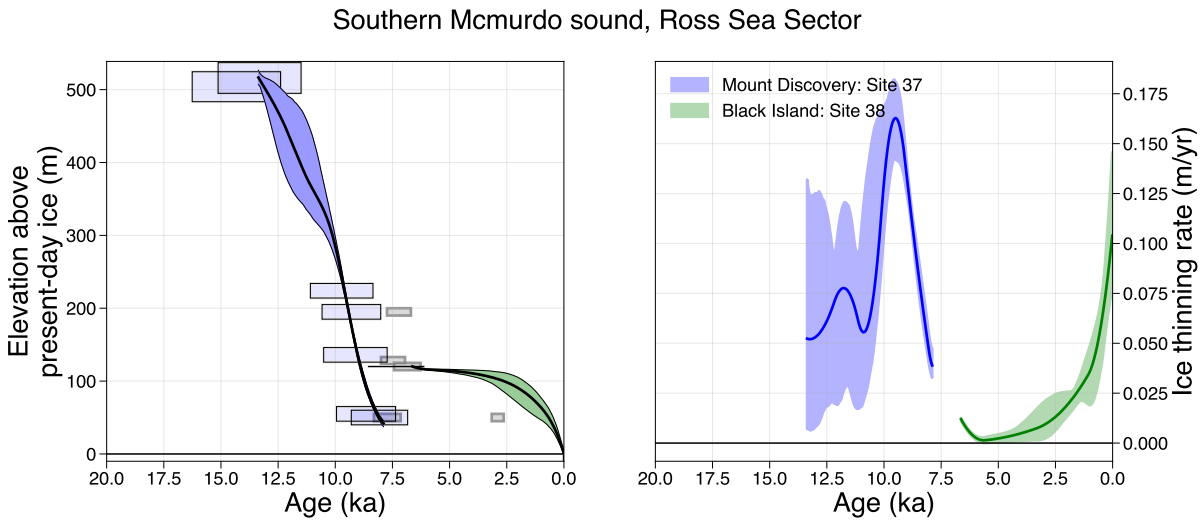

Fig. S27 Thinning histories from Southern Mcmurdo Sound Ross Sea Sector. Colored boxes mark cosmogenic nuclide exposure age data and/or radiocarbon-dated lakes. Gray boxes mark rejected data. Colored envelopes denote PATR median and 95% credible intervals for local Antarctic Ice Sheet elevation (left panel) and rate of thinning (right panel).

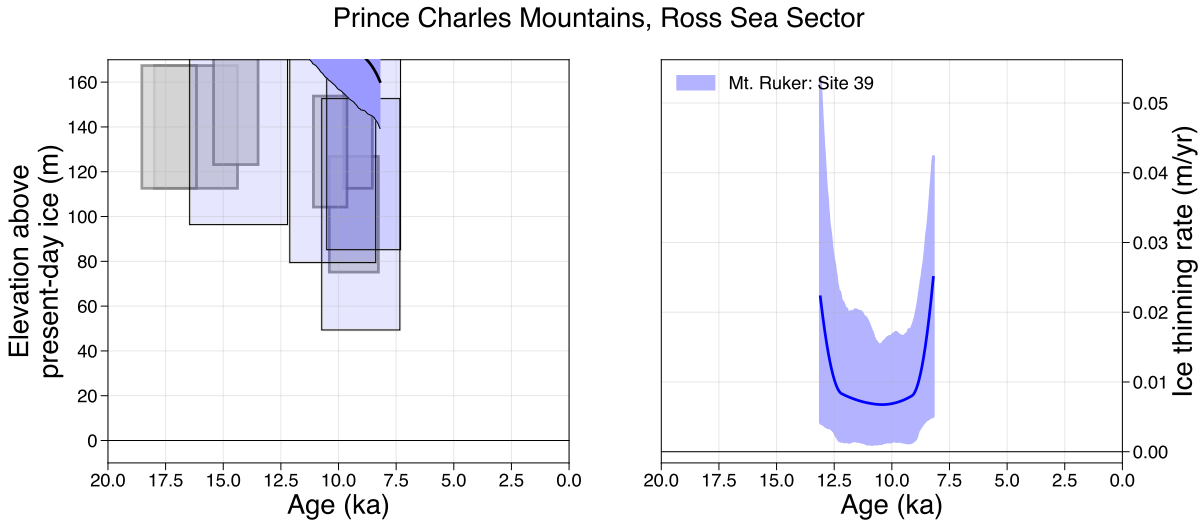

Fig. S28 Thinning histories from Prince Charles Mountains Ross Sea Sector. Colored boxes mark cosmogenic nuclide exposure age data and/or radiocarbon-dated lakes. Gray boxes mark rejected data. Colored envelopes denote PATR median and 95% credible intervals for local Antarctic Ice Sheet elevation (left panel) and rate of thinning (right panel).

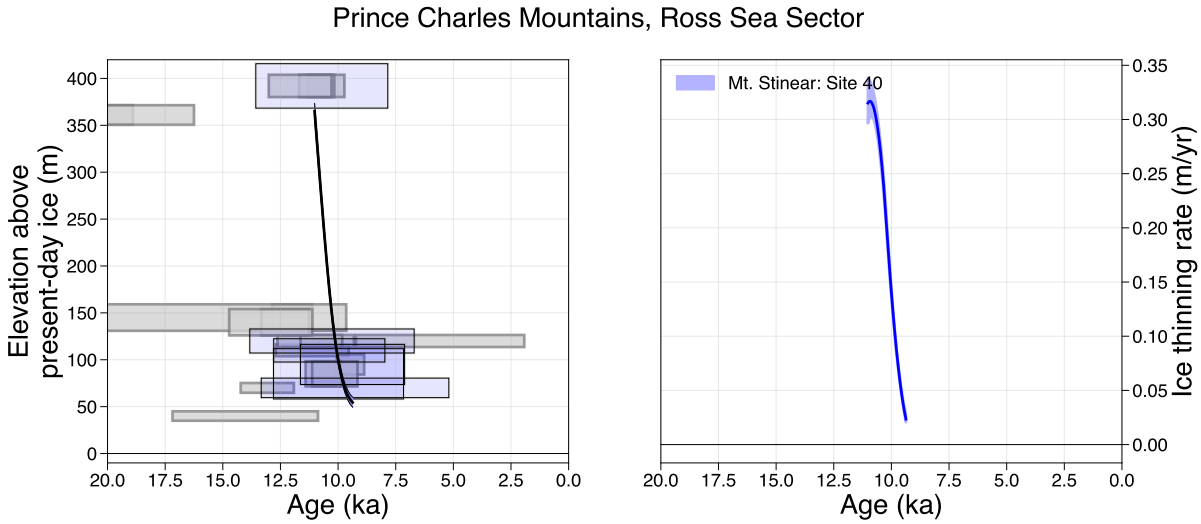

Fig. S29 Thinning histories from Prince Charles Mountains Ross Sea Sector. Colored boxes mark cosmogenic nuclide exposure age data and/or radiocarbon-dated lakes. Gray boxes mark rejected data. Colored envelopes denote PATR median and 95% credible intervals for local Antarctic Ice Sheet elevation (left panel) and rate of thinning (right panel).

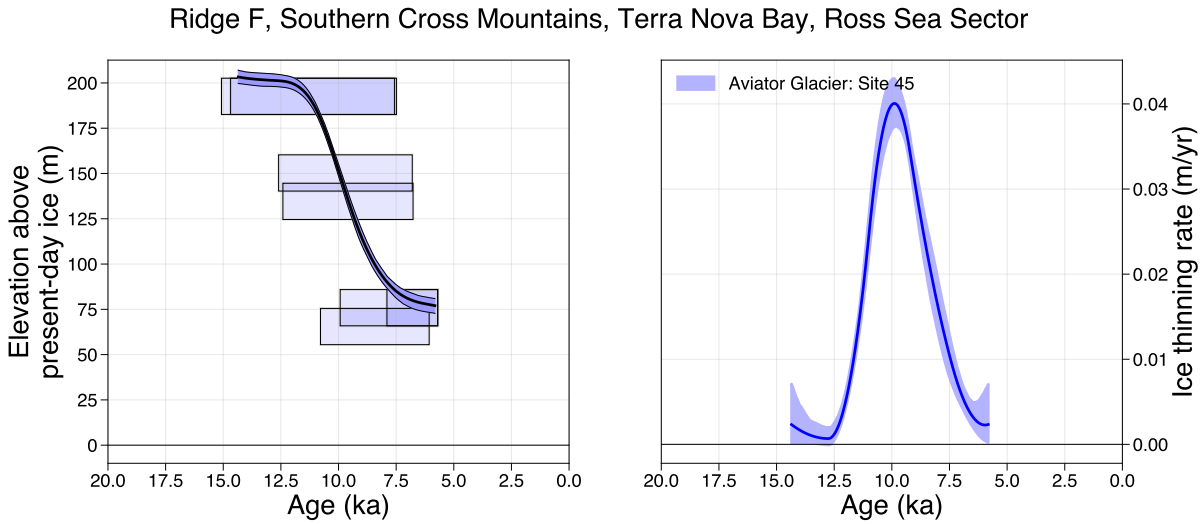

Fig. S30 Thinning histories from Ridge F Southern Cross Mountains Terra Nova Bay Ross Sea Sector. Colored boxes mark cosmogenic nuclide exposure age data and/or radiocarbon-dated lakes. Gray boxes mark rejected data. Colored envelopes denote PATR median and 95% credible intervals for local Antarctic Ice Sheet elevation (left panel) and rate of thinning (right panel).

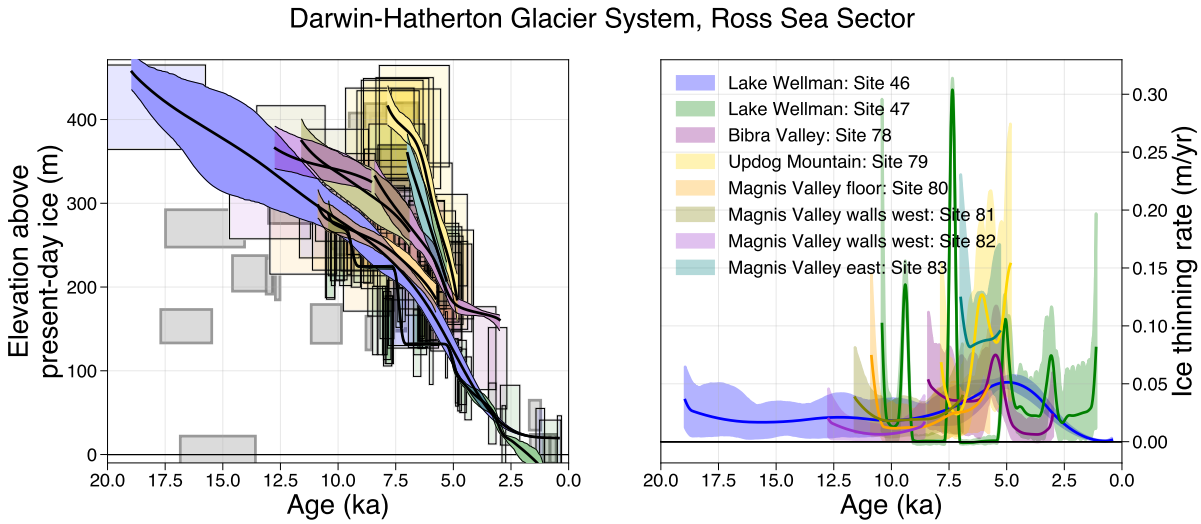

Fig. S31 Thinning histories from Darwin-Hatherton Glacier System Ross Sea Sector. Colored boxes mark cosmogenic nuclide exposure age data and/or radiocarbon-dated lakes. Gray boxes mark rejected data. Colored envelopes denote PATR median and 95% credible intervals for local Antarctic Ice Sheet elevation (left panel) and rate of thinning (right panel).

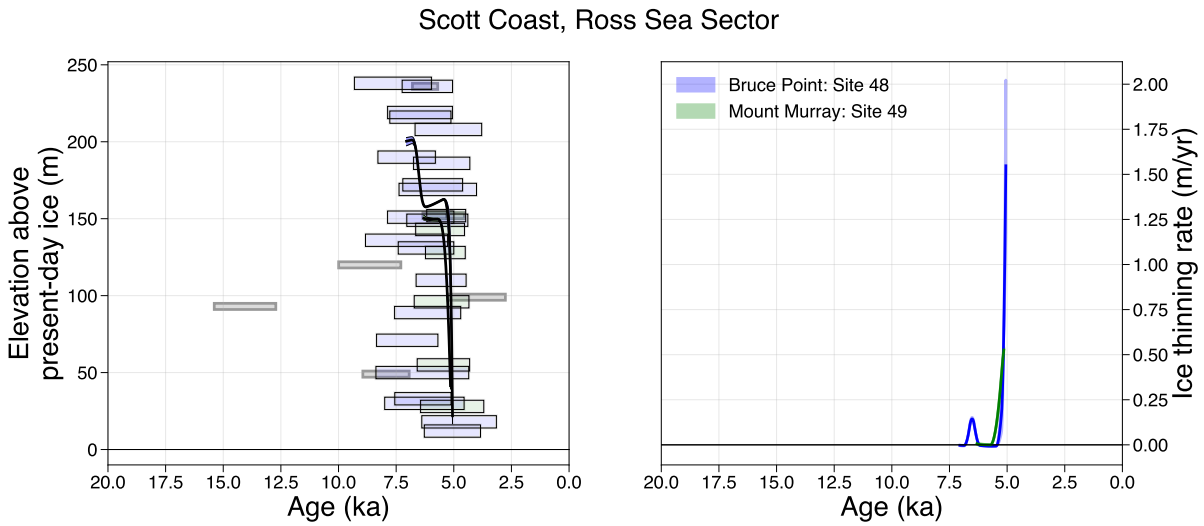

Fig. S32 Thinning histories from Scott Coast Ross Sea Sector. Colored boxes mark cosmogenic nuclide exposure age data and/or radiocarbon-dated lakes. Gray boxes mark rejected data. Colored envelopes denote PATR median and 95% credible intervals for local Antarctic Ice Sheet elevation (left panel) and rate of thinning (right panel).

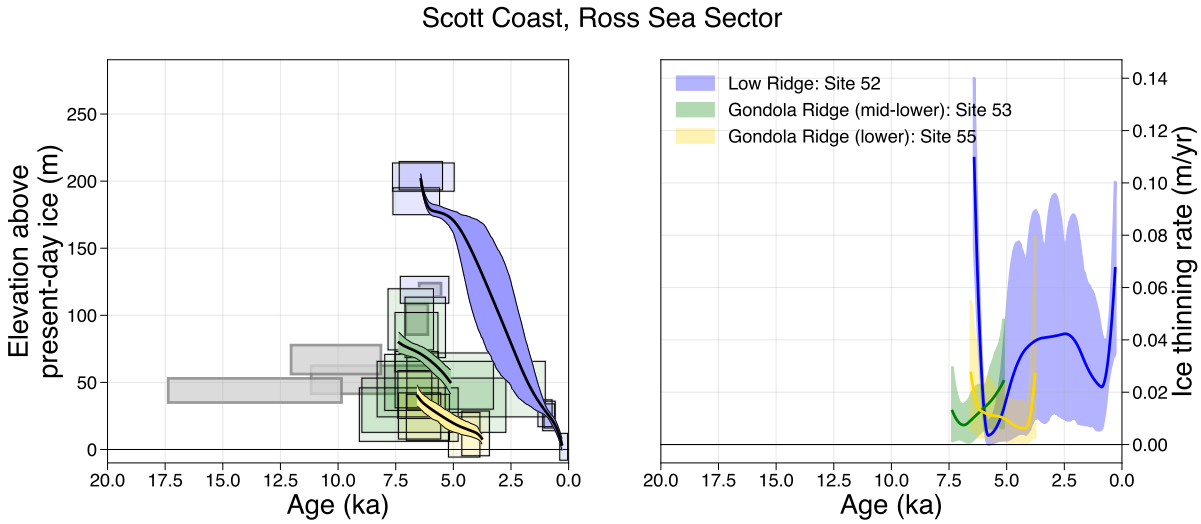

Fig. S33 Thinning histories from Scott Coast Ross Sea Sector. Colored boxes mark cosmogenic nuclide exposure age data and/or radiocarbon-dated lakes. Gray boxes mark rejected data. Colored envelopes denote PATR median and 95% credible intervals for local Antarctic Ice Sheet elevation (left panel) and rate of thinning (right panel).

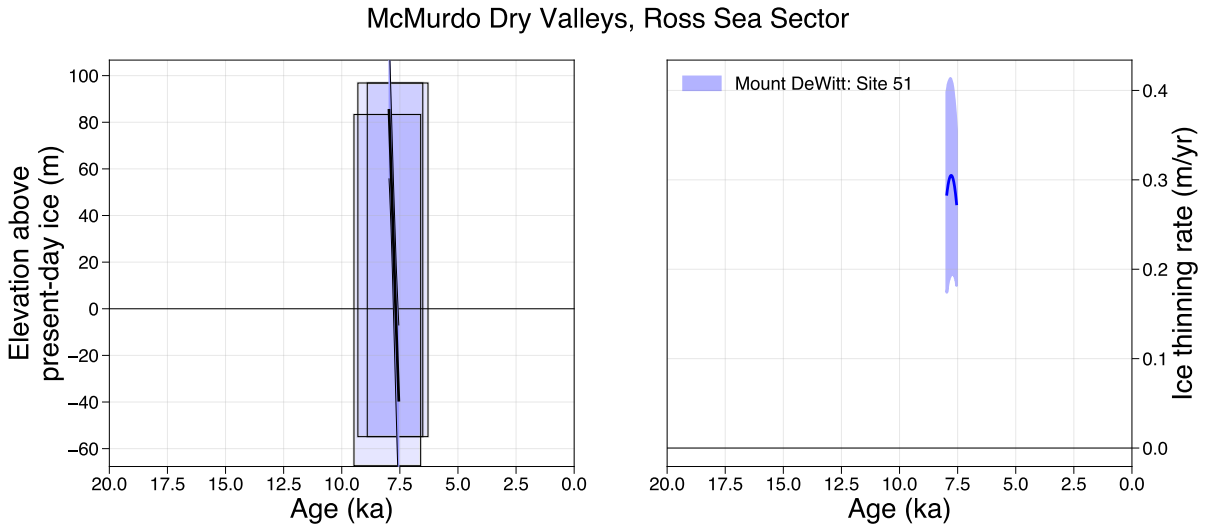

Fig. S34 Thinning histories from McMurdo Dry Valleys Ross Sea Sector. Colored boxes mark cosmogenic nuclide exposure age data and/or radiocarbon-dated lakes. Gray boxes mark rejected data. Colored envelopes denote PATR median and 95% credible intervals for local Antarctic Ice Sheet elevation (left panel) and rate of thinning (right panel).

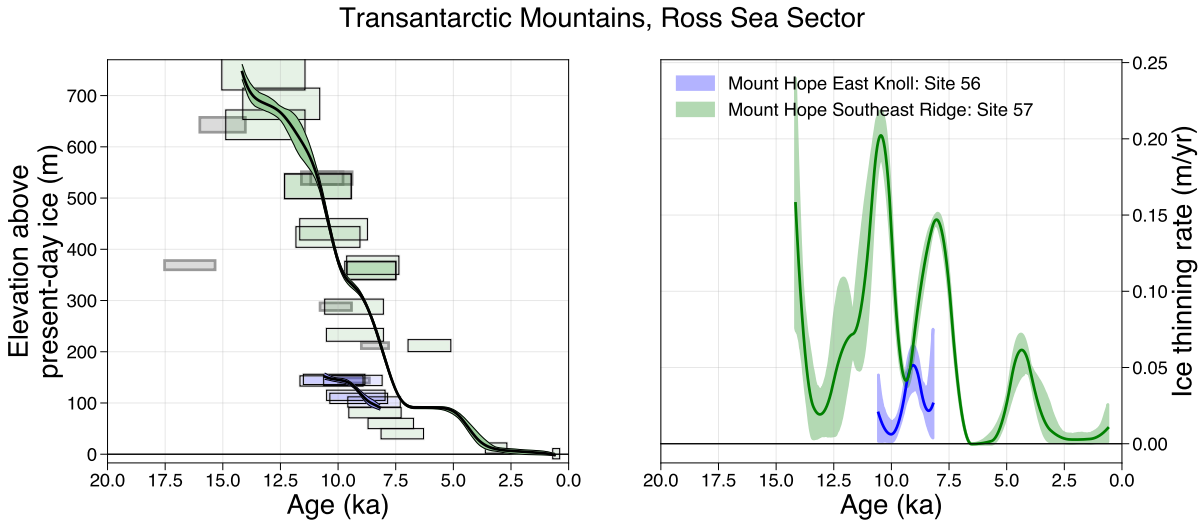

Fig. S35 Thinning histories from Transantarctic Mountains Ross Sea Sector. Colored boxes mark cosmogenic nuclide exposure age data and/or radiocarbon-dated lakes. Gray boxes mark rejected data. Colored envelopes denote PATR median and 95% credible intervals for local Antarctic Ice Sheet elevation (left panel) and rate of thinning (right panel).

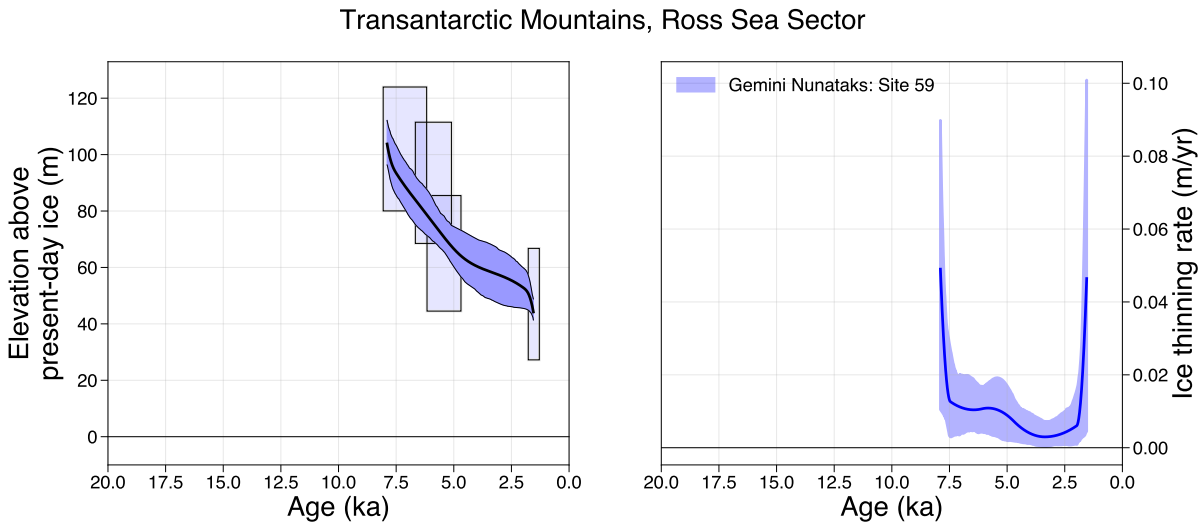

Fig. S36 Thinning histories from Transantarctic Mountains Ross Sea Sector. Colored boxes mark cosmogenic nuclide exposure age data and/or radiocarbon-dated lakes. Gray boxes mark rejected data. Colored envelopes denote PATR median and 95% credible intervals for local Antarctic Ice Sheet elevation (left panel) and rate of thinning (right panel).

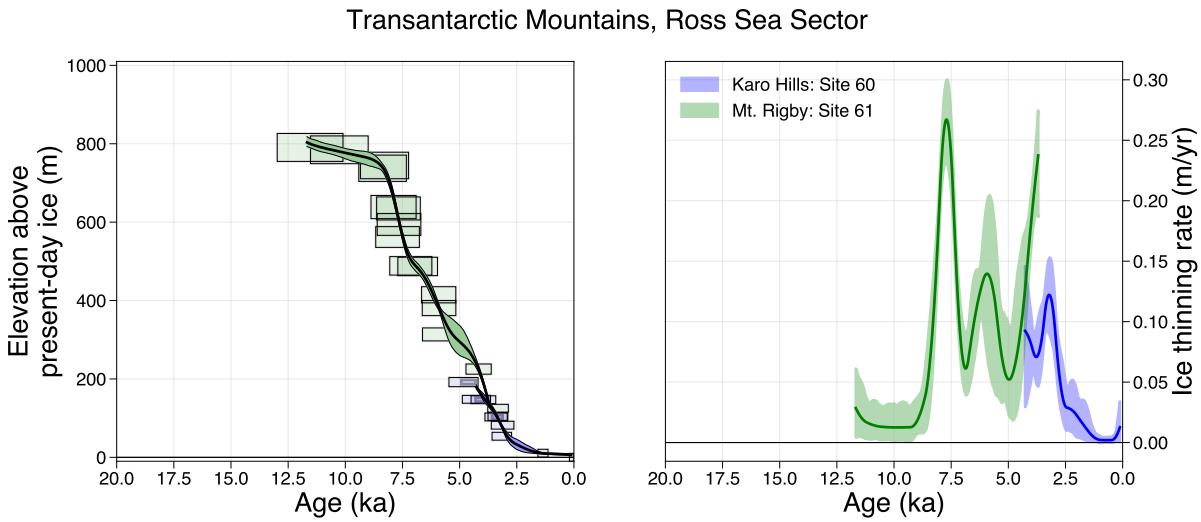

Fig. S37 Thinning histories from Transantarctic Mountains Ross Sea Sector. Colored boxes mark cosmogenic nuclide exposure age data and/or radiocarbon-dated lakes. Gray boxes mark rejected data. Colored envelopes denote PATR median and 95% credible intervals for local Antarctic Ice Sheet elevation (left panel) and rate of thinning (right panel).

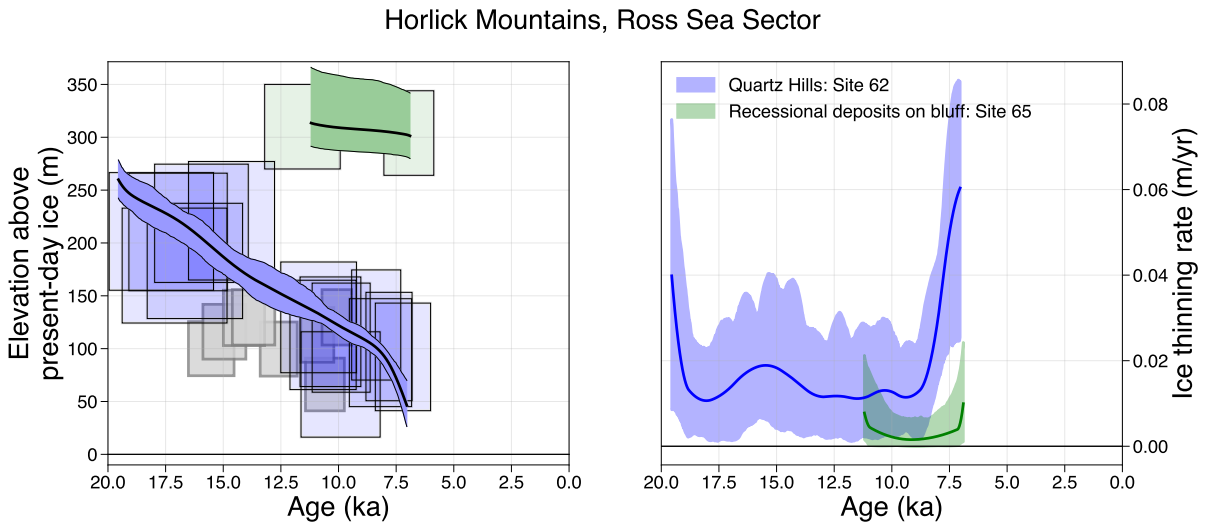

Fig. S38 Thinning histories from Horlick Mountains Ross Sea Sector. Colored boxes mark cosmogenic nuclide exposure age data and/or radiocarbon-dated lakes. Gray boxes mark rejected data. Colored envelopes denote PATR median and 95% credible intervals for local Antarctic Ice Sheet elevation (left panel) and rate of thinning (right panel).

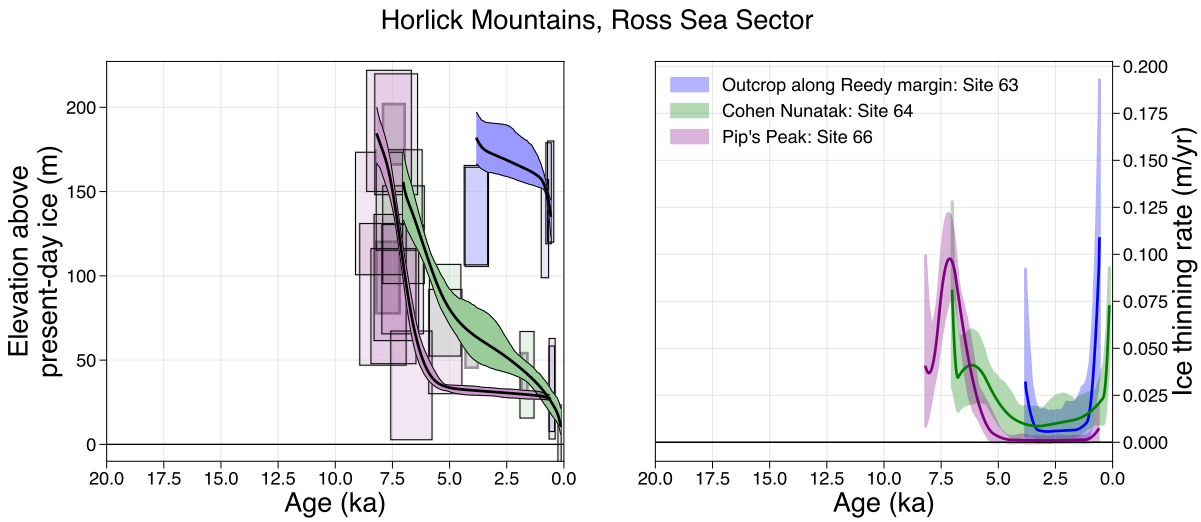

Fig. S39 Thinning histories from Horlick Mountains Ross Sea Sector. Colored boxes mark cosmogenic nuclide exposure age data and/or radiocarbon-dated lakes. Gray boxes mark rejected data. Colored envelopes denote PATR median and 95% credible intervals for local Antarctic Ice Sheet elevation (left panel) and rate of thinning (right panel).

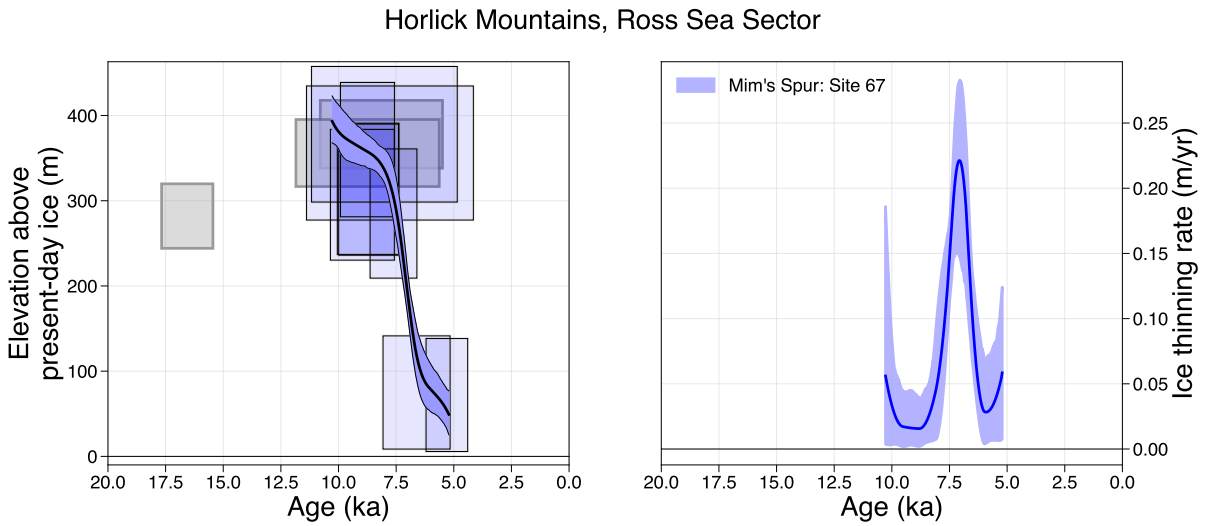

Fig. S40 Thinning histories from Horlick Mountains Ross Sea Sector. Colored boxes mark cosmogenic nuclide exposure age data and/or radiocarbon-dated lakes. Gray boxes mark rejected data. Colored envelopes denote PATR median and 95% credible intervals for local Antarctic Ice Sheet elevation (left panel) and rate of thinning (right panel).

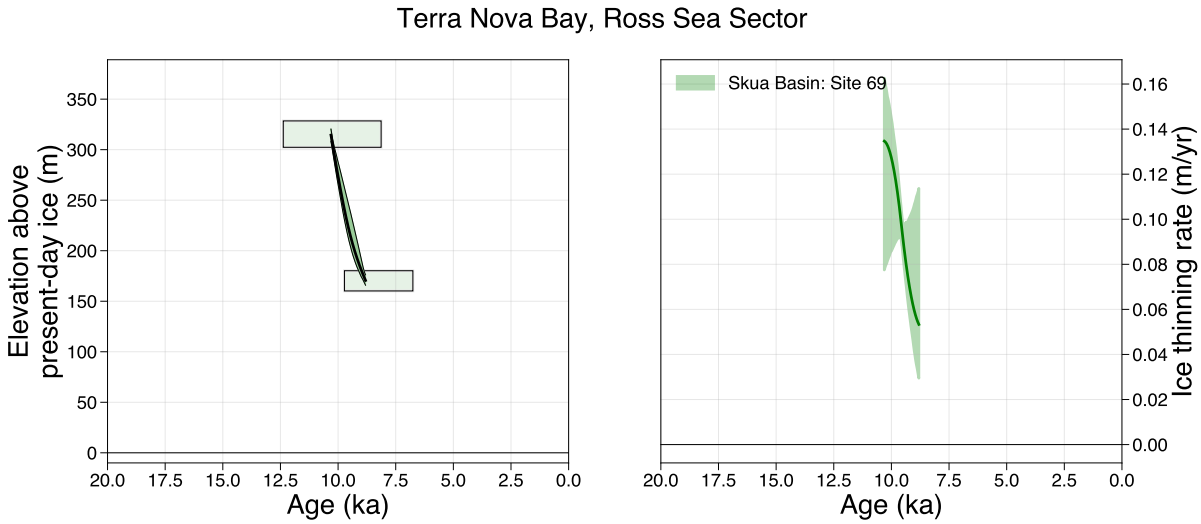

Fig. S41 Thinning histories from Terra Nova Bay Ross SEa Sector. Colored boxes mark cosmogenic nuclide exposure age data and/or radiocarbon-dated lakes. Gray boxes mark rejected data. Colored envelopes denote PATR median and 95% credible intervals for local Antarctic Ice Sheet elevation (left panel) and rate of thinning (right panel).

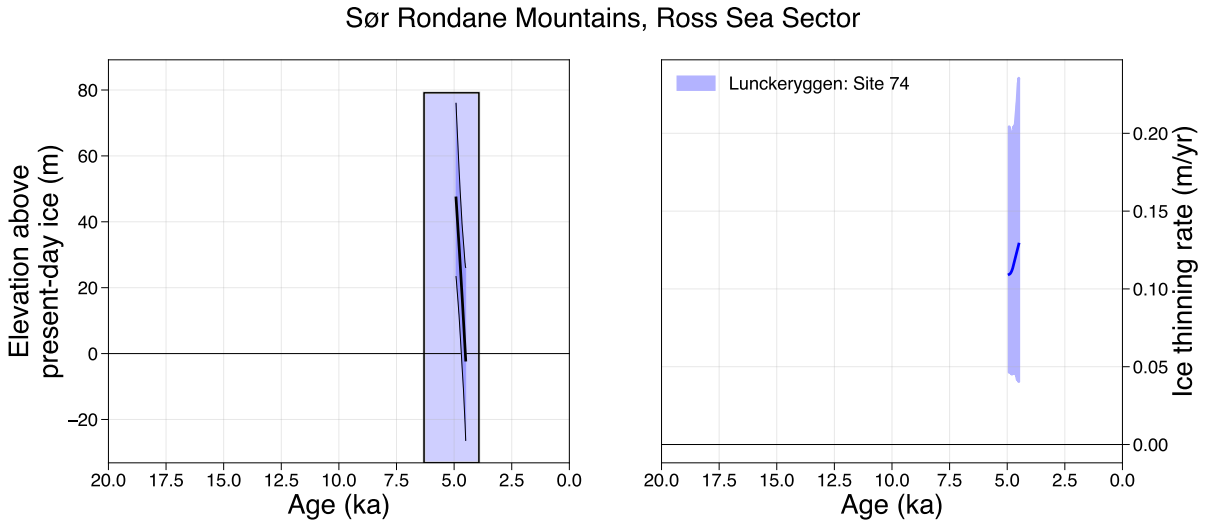

Fig. S42 Thinning histories from Sør Rondane Mountains Ross Sea Sector. Colored boxes mark cosmogenic nuclide exposure age data and/or radiocarbon-dated lakes. Gray boxes mark rejected data. Colored envelopes denote PATR median and 95% credible intervals for local Antarctic Ice Sheet elevation (left panel) and rate of thinning (right panel).

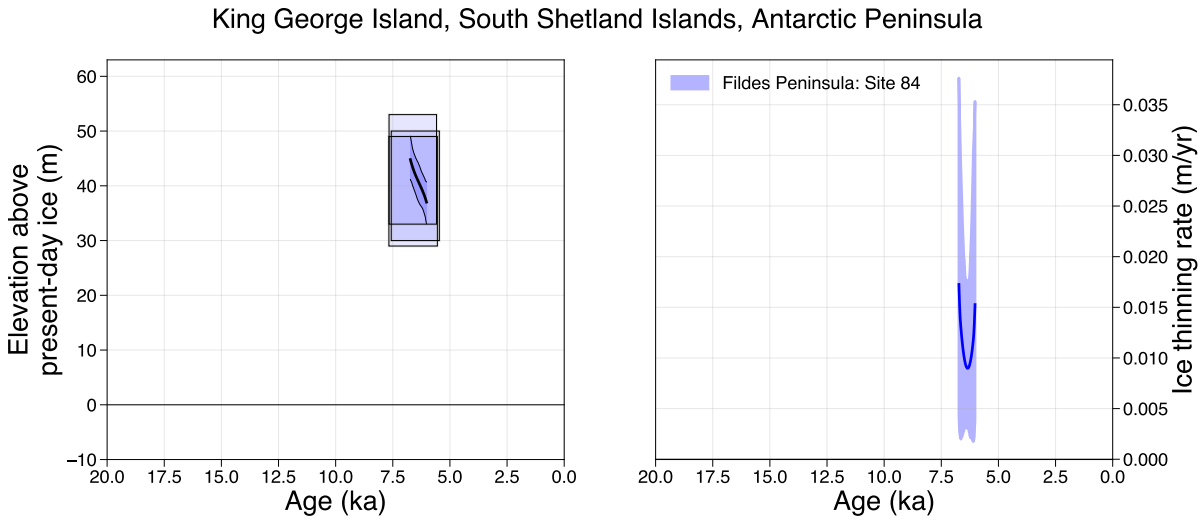

Fig. S43 Thinning histories from King George Island South Shetland Islands Antarctic Peninsula. Colored boxes mark cosmogenic nuclide exposure age data and/or radiocarbon-dated lakes. Gray boxes mark rejected data. Colored envelopes denote PATR median and 95% credible intervals for local Antarctic Ice Sheet elevation (left panel) and rate of thinning (right panel).

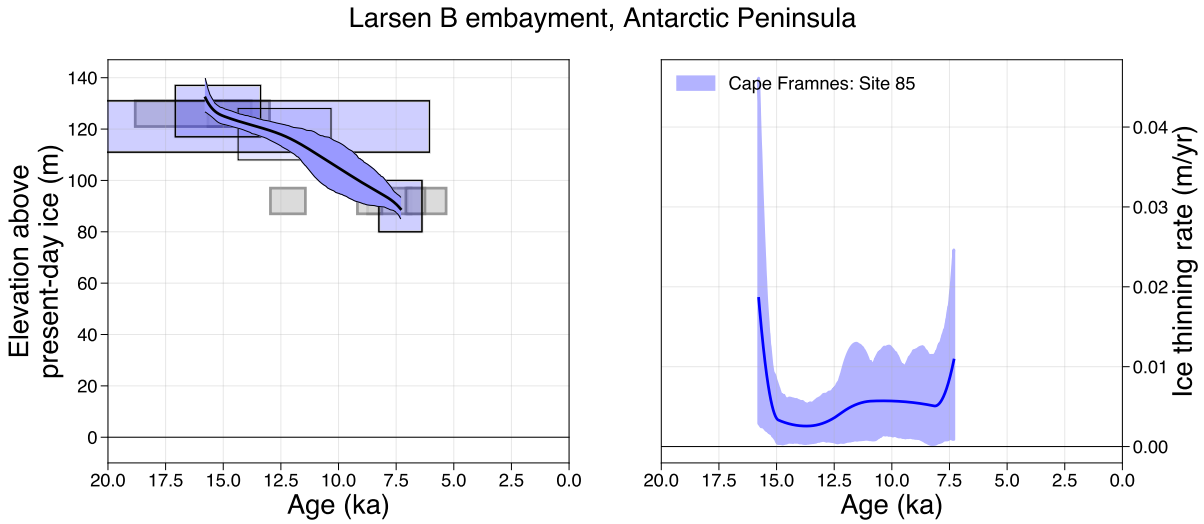

Fig. S44 Thinning histories from Larsen B Embayment Antarctic Peninsula. Colored boxes mark cosmogenic nuclide exposure age data and/or radiocarbon-dated lakes. Gray boxes mark rejected data. Colored envelopes denote PATR median and 95% credible intervals for local Antarctic Ice Sheet elevation (left panel) and rate of thinning (right panel).

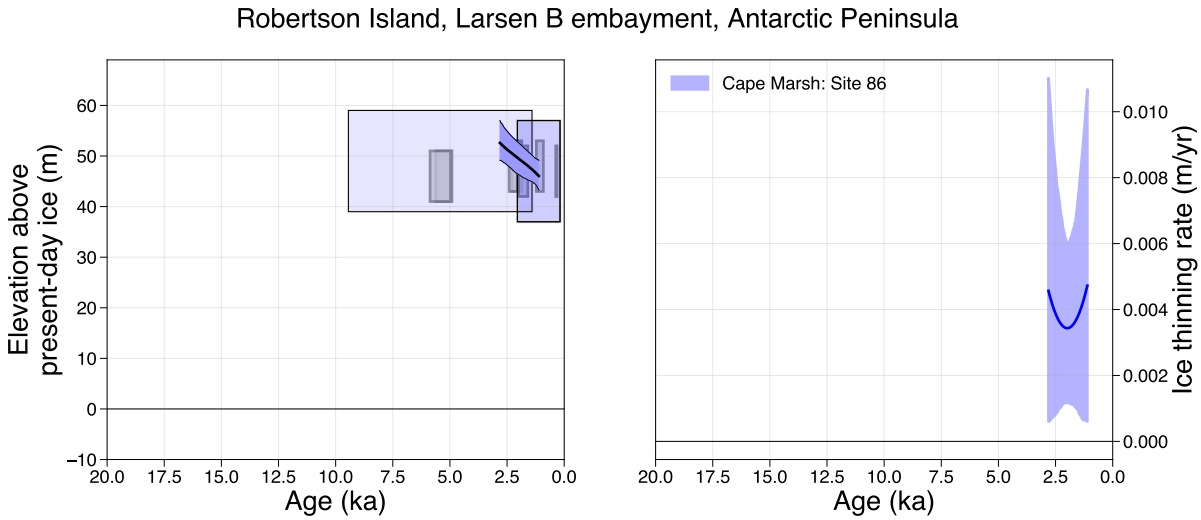

Fig. S45 Thinning histories from Robertson Island Larsen B Embayment Antarctic Peninsula. Colored boxes mark cosmogenic nuclide exposure age data and/or radiocarbon-dated lakes. Gray boxes mark rejected data. Colored envelopes denote PATR median and 95% credible intervals for local Antarctic Ice Sheet elevation (left panel) and rate of thinning (right panel).

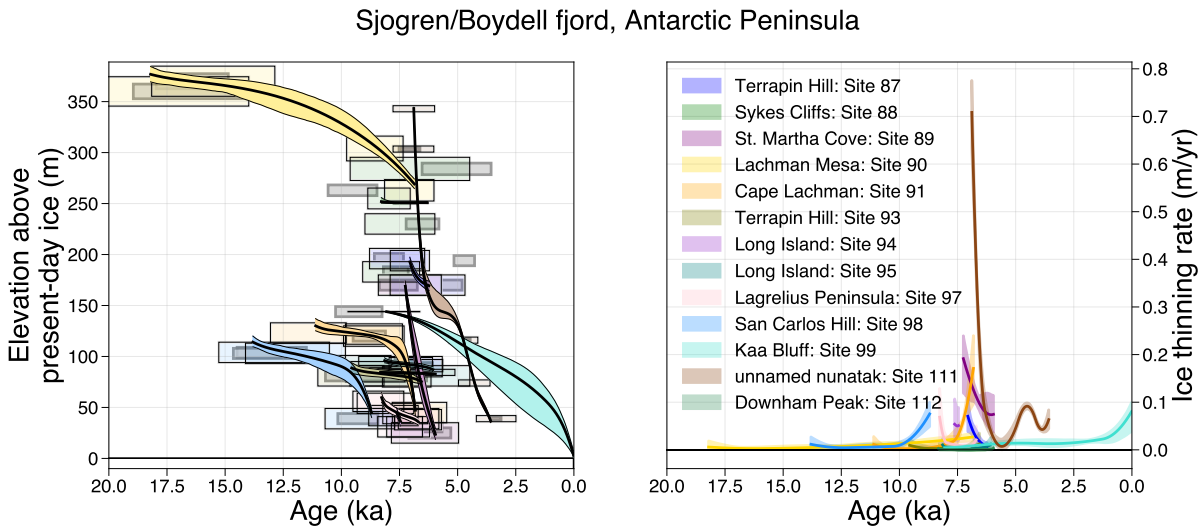

Fig. S46 Thinning histories from SjogrenBoydell fjord Antarctic Peninsula. Colored boxes mark cosmogenic nuclide exposure age data and/or radiocarbon-dated lakes. Gray boxes mark rejected data. Colored envelopes denote PATR median and 95% credible intervals for local Antarctic Ice Sheet elevation (left panel) and rate of thinning (right panel).

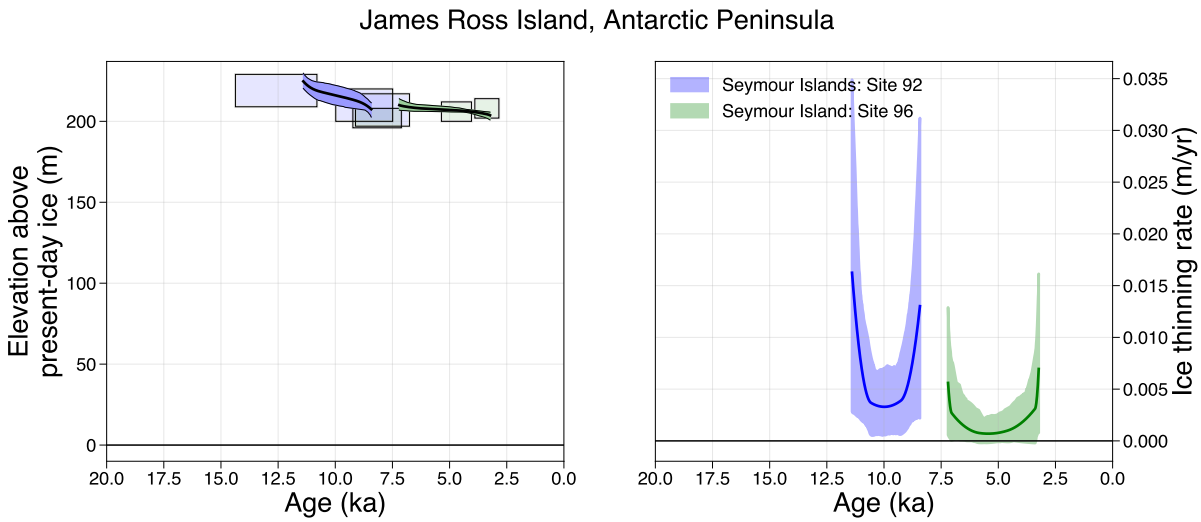

Fig. S47 Thinning histories from James Ross Island Antarctic Peninsula. Colored boxes mark cosmogenic nuclide exposure age data and/or radiocarbon-dated lakes. Gray boxes mark rejected data. Colored envelopes denote PATR median and 95% credible intervals for local Antarctic Ice Sheet elevation (left panel) and rate of thinning (right panel).

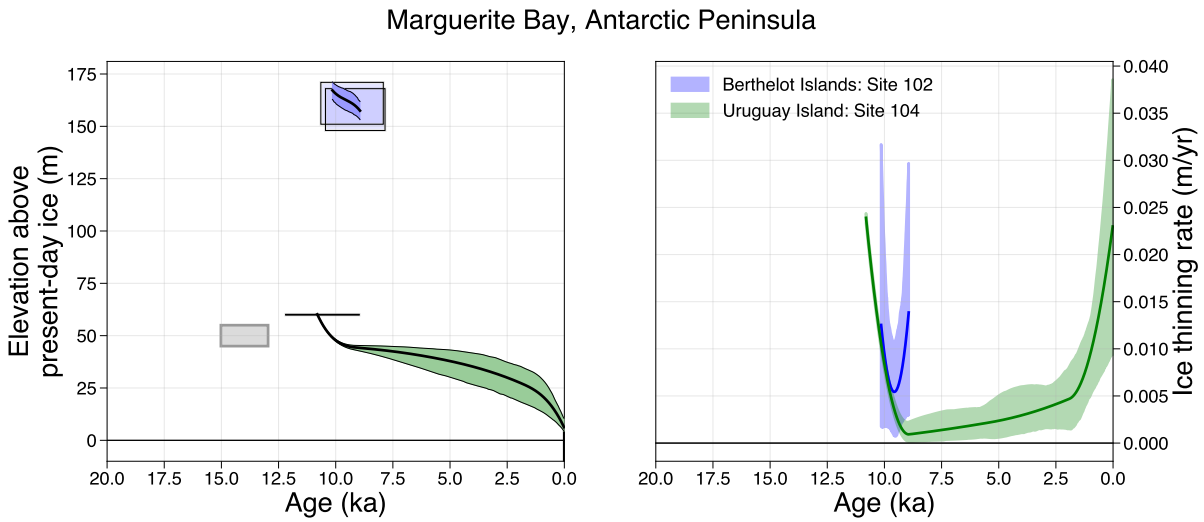

Fig. S48 Thinning histories from Marguerite Bay Antarctic Peninsula. Colored boxes mark cosmogenic nuclide exposure age data and/or radiocarbon-dated lakes. Gray boxes mark rejected data. Colored envelopes denote PATR median and 95% credible intervals for local Antarctic Ice Sheet elevation (left panel) and rate of thinning (right panel).

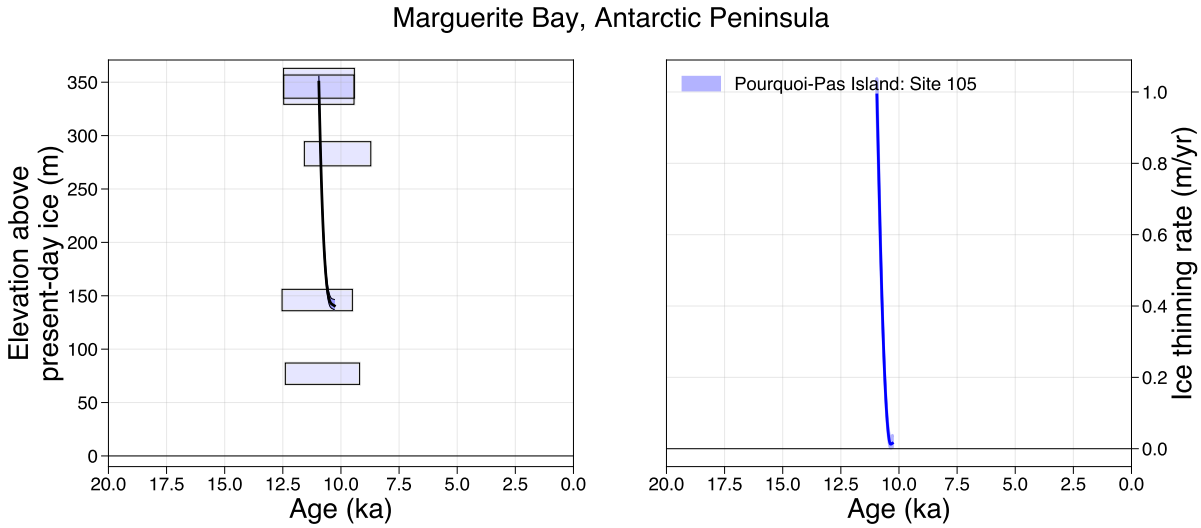

Fig. S49 Thinning histories from Marguerite Bay Antarctic Peninsula. Colored boxes mark cosmogenic nuclide exposure age data and/or radiocarbon-dated lakes. Gray boxes mark rejected data. Colored envelopes denote PATR median and 95% credible intervals for local Antarctic Ice Sheet elevation (left panel) and rate of thinning (right panel).

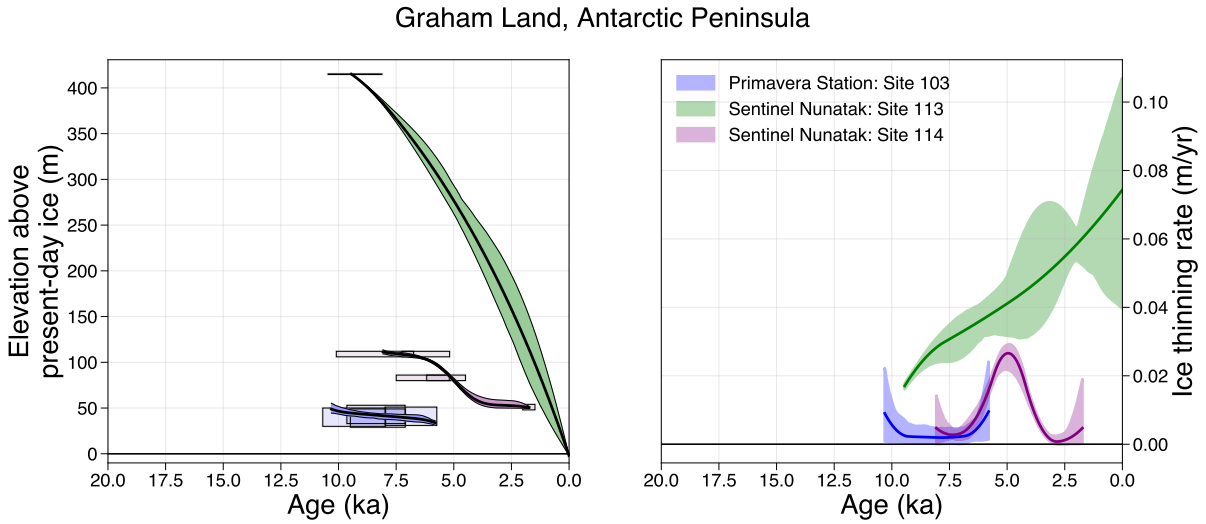

Fig. S50 Thinning histories from Graham Land Antarctic Peninsula. Colored boxes mark cosmogenic nuclide exposure age data and/or radiocarbon-dated lakes. Gray boxes mark rejected data. Colored envelopes denote PATR median and 95% credible intervals for local Antarctic Ice Sheet elevation (left panel) and rate of thinning (right panel).

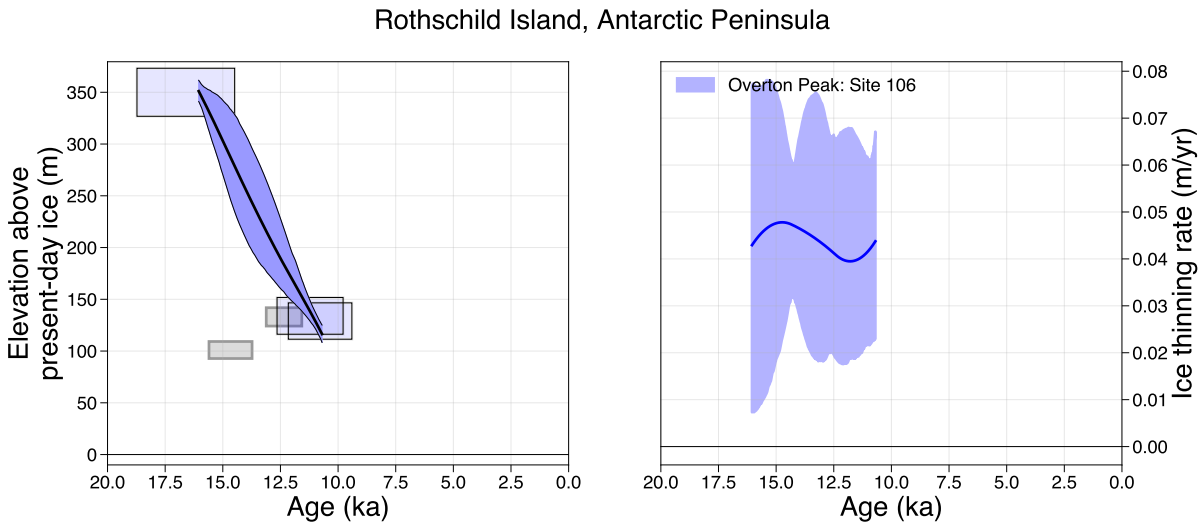

Fig. S51 Thinning histories from Rothschild Island Antarctic Peninsula. Colored boxes mark cosmogenic nuclide exposure age data and/or radiocarbon-dated lakes. Gray boxes mark rejected data. Colored envelopes denote PATR median and 95% credible intervals for local Antarctic Ice Sheet elevation (left panel) and rate of thinning (right panel).

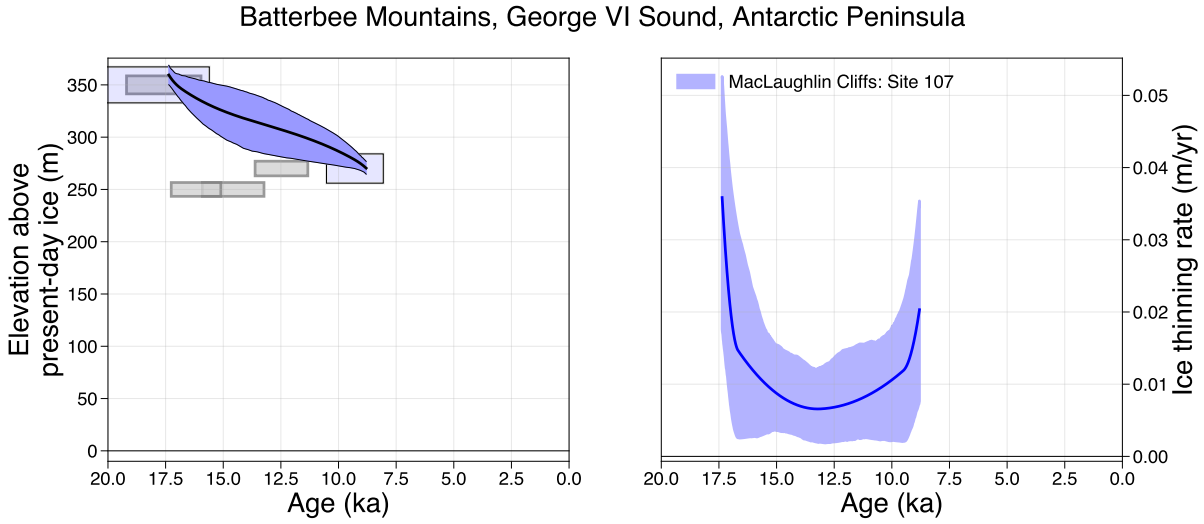

Fig. S52 Thinning histories from Batterbee Mountains George VI Sound Antarctic Peninsula. Colored boxes mark cosmogenic nuclide exposure age data and/or radiocarbon-dated lakes. Gray boxes mark rejected data. Colored envelopes denote PATR median and 95% credible intervals for local Antarctic Ice Sheet elevation (left panel) and rate of thinning (right panel).

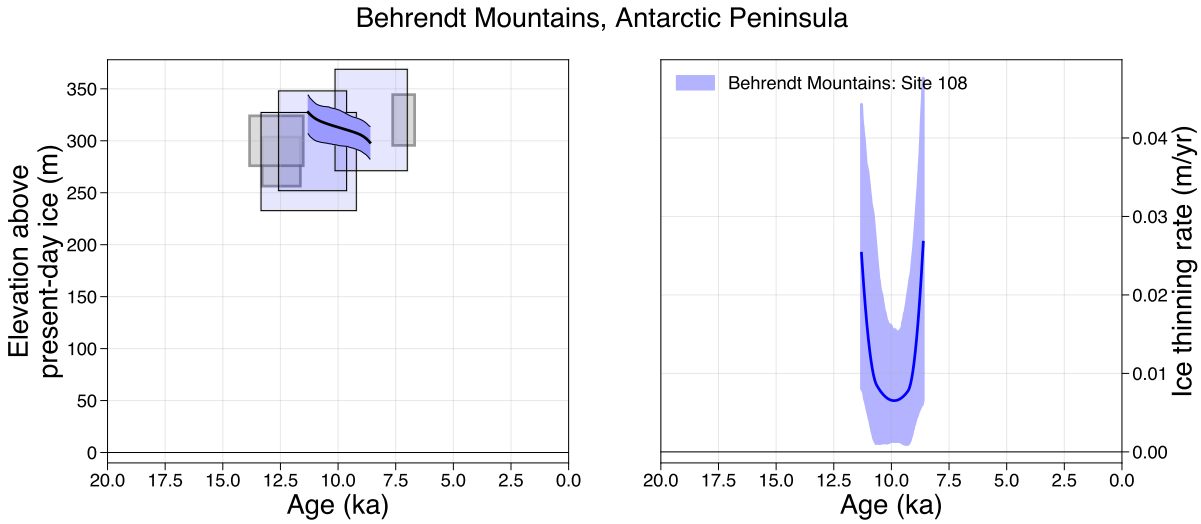

Fig. S53 Thinning histories from Behrendt Mountains Antarctic Peninsula. Colored boxes mark cosmogenic nuclide exposure age data and/or radiocarbon-dated lakes. Gray boxes mark rejected data. Colored envelopes denote PATR median and 95% credible intervals for local Antarctic Ice Sheet elevation (left panel) and rate of thinning (right panel).

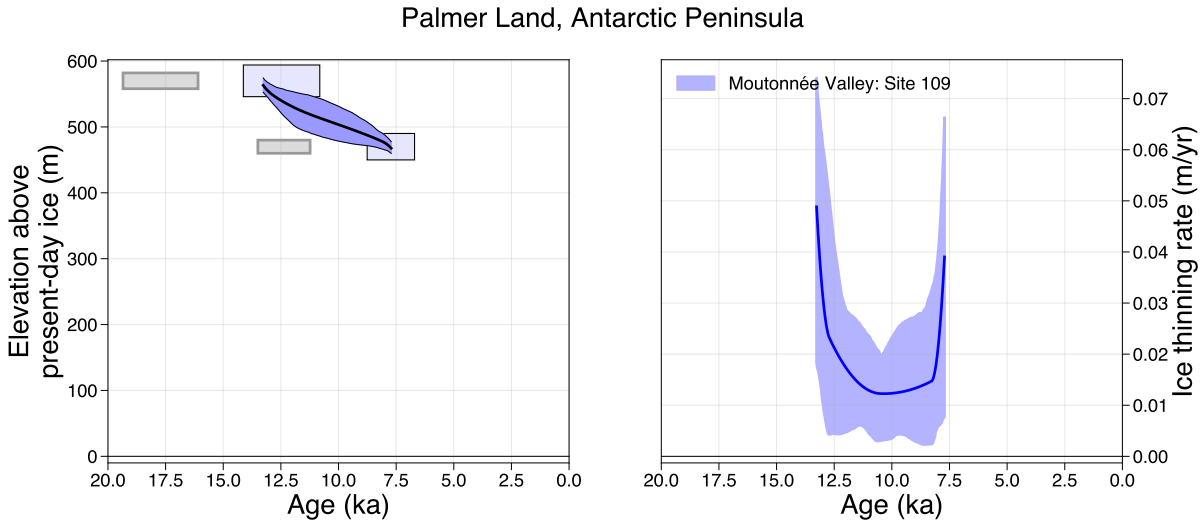

Fig. S54 Thinning histories from Palmer Land Antarctic Peninsula. Colored boxes mark cosmogenic nuclide exposure age data and/or radiocarbon-dated lakes. Gray boxes mark rejected data. Colored envelopes denote PATR median and 95% credible intervals for local Antarctic Ice Sheet elevation (left panel) and rate of thinning (right panel).

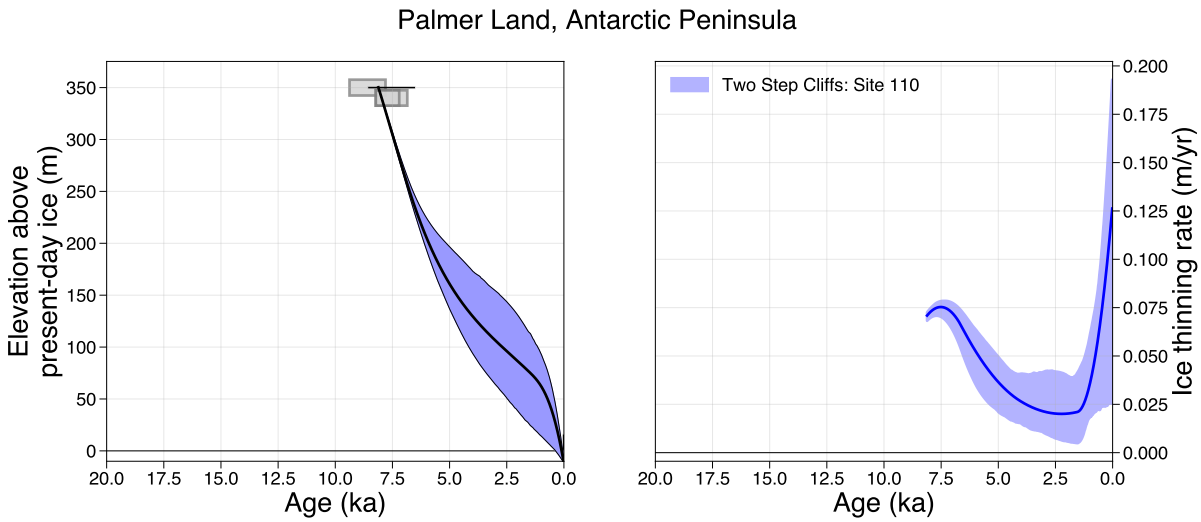

Fig. S55 Thinning histories from Palmer Land Antarctic Peninsula. Colored boxes mark cosmogenic nuclide exposure age data and/or radiocarbon-dated lakes. Gray boxes mark rejected data. Colored envelopes denote PATR median and 95% credible intervals for local Antarctic Ice Sheet elevation (left panel) and rate of thinning (right panel).

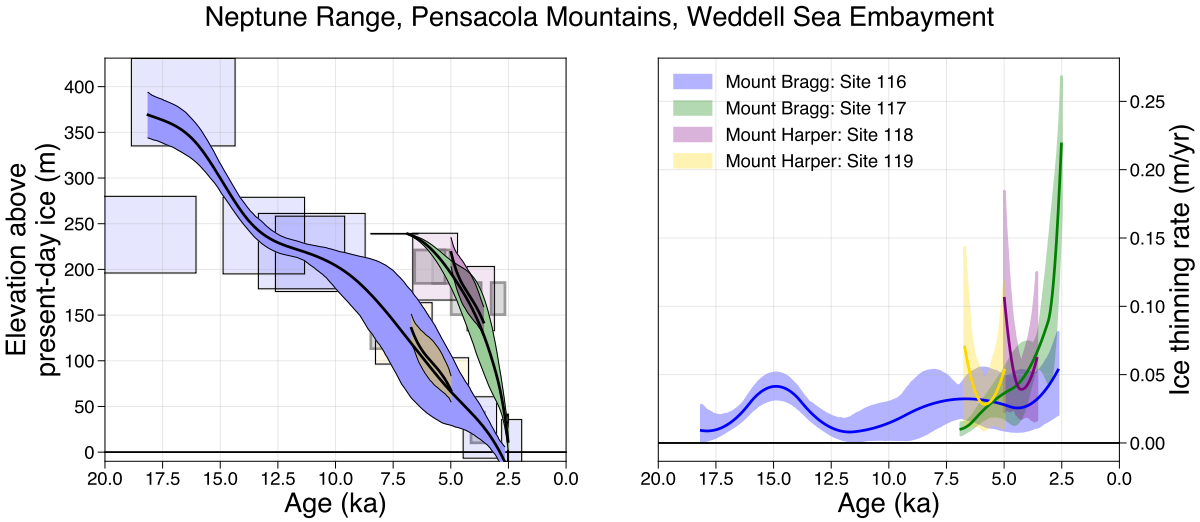

Fig. S56 Thinning histories from Neptune Range Pensacola Mountains Weddell Sea Embayment. Colored boxes mark cosmogenic nuclide exposure age data and/or radiocarbon-dated lakes. Gray boxes mark rejected data. Colored envelopes denote PATR median and 95% credible intervals for local Antarctic Ice Sheet elevation (left panel) and rate of thinning (right panel).

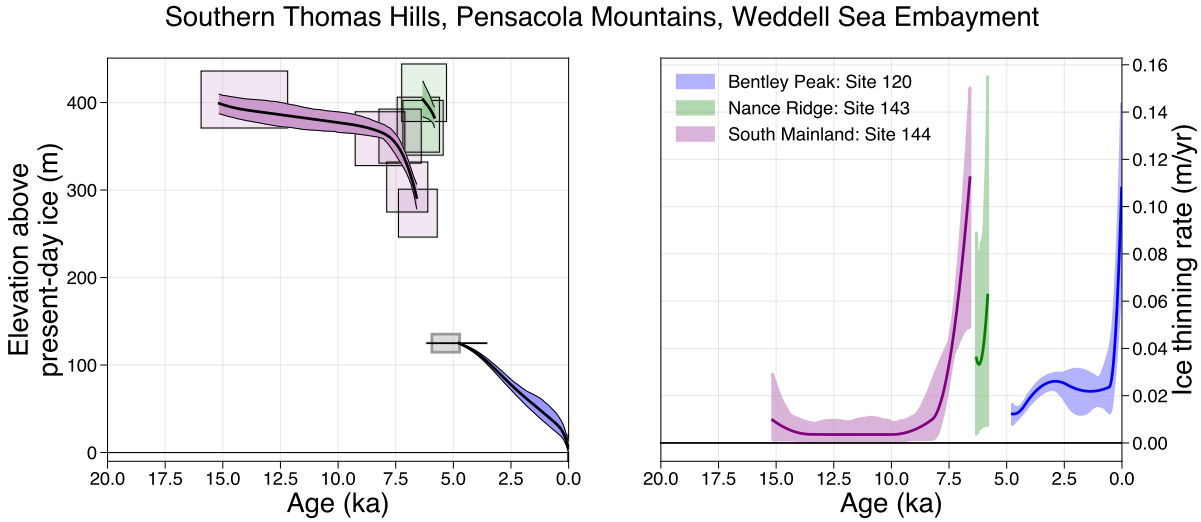

Fig. S57 Thinning histories from Southern Thomas Hills Pensacola Mountains Weddell Sea Embayment. Colored boxes mark cosmogenic nuclide exposure age data and/or radiocarbon-dated lakes. Gray boxes mark rejected data. Colored envelopes denote PATR median and 95% credible intervals for local Antarctic Ice Sheet elevation (left panel) and rate of thinning (right panel).

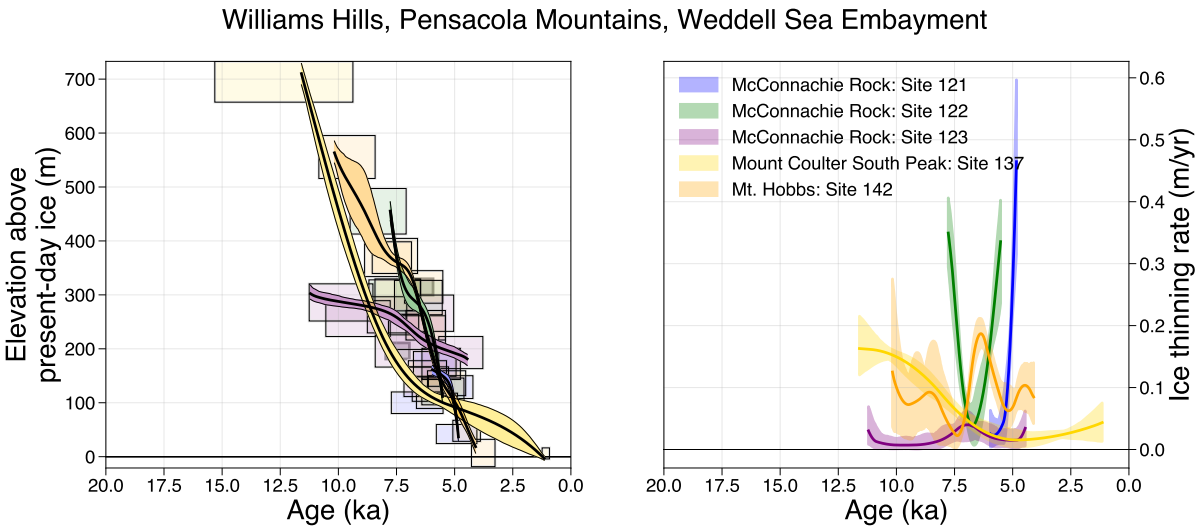

Fig. S58 Thinning histories from Williams Hills Pensacola Mountains Weddell Sea Embayment. Colored boxes mark cosmogenic nuclide exposure age data and/or radiocarbon-dated lakes. Gray boxes mark rejected data. Colored envelopes denote PATR median and 95% credible intervals for local Antarctic Ice Sheet elevation (left panel) and rate of thinning (right panel).

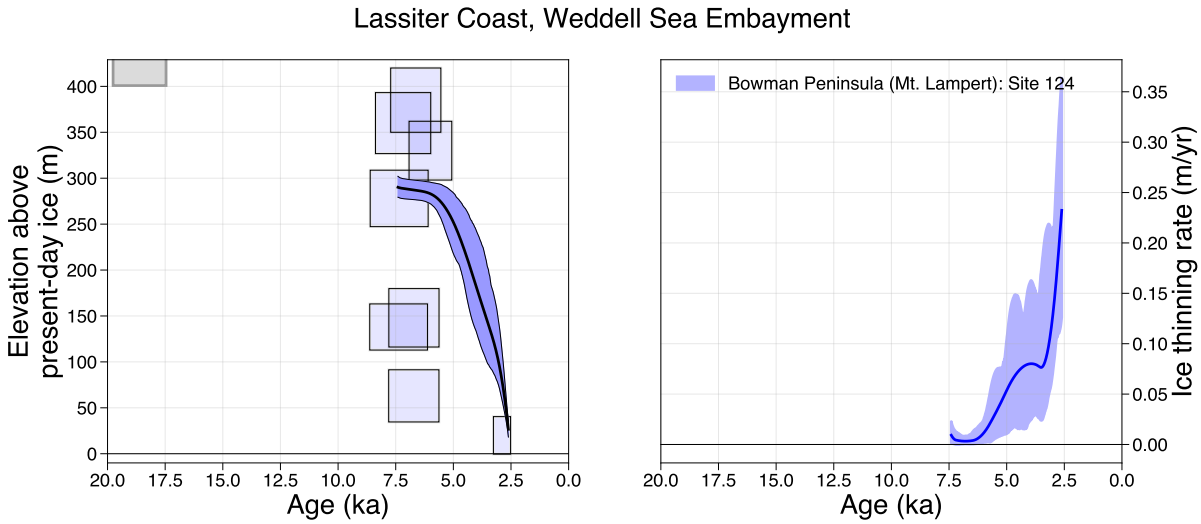

Fig. S59 Thinning histories from Lassiter Coast Weddell Sea Embayment. Colored boxes mark cosmogenic nuclide exposure age data and/or radiocarbon-dated lakes. Gray boxes mark rejected data. Colored envelopes denote PATR median and 95% credible intervals for local Antarctic Ice Sheet elevation (left panel) and rate of thinning (right panel).

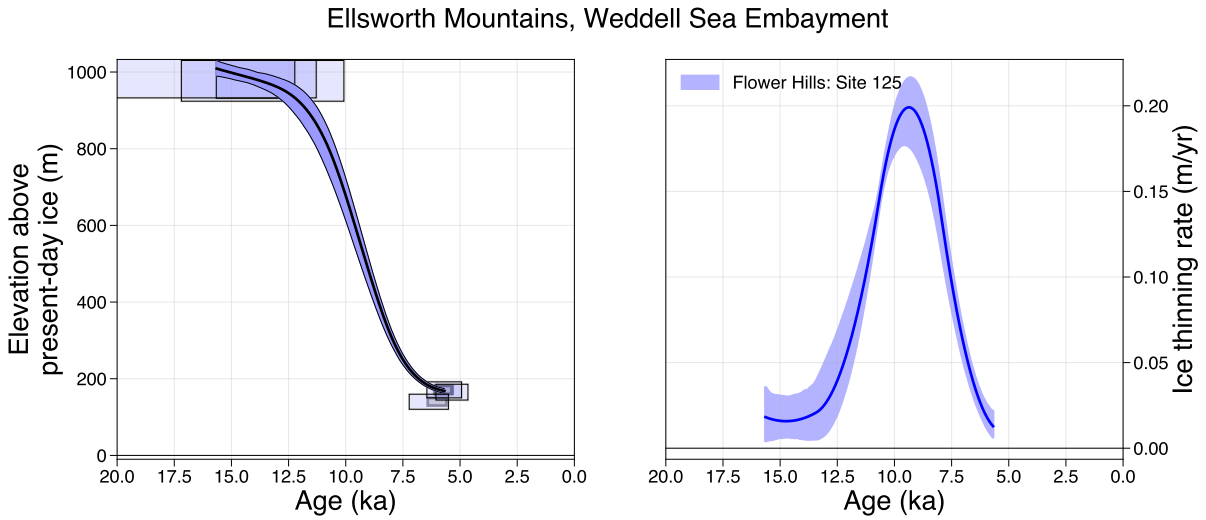

Fig. S60 Thinning histories from Ellsworth Mountains Weddell Sea Embayment. Colored boxes mark cosmogenic nuclide exposure age data and/or radiocarbon-dated lakes. Gray boxes mark rejected data. Colored envelopes denote PATR median and 95% credible intervals for local Antarctic Ice Sheet elevation (left panel) and rate of thinning (right panel).

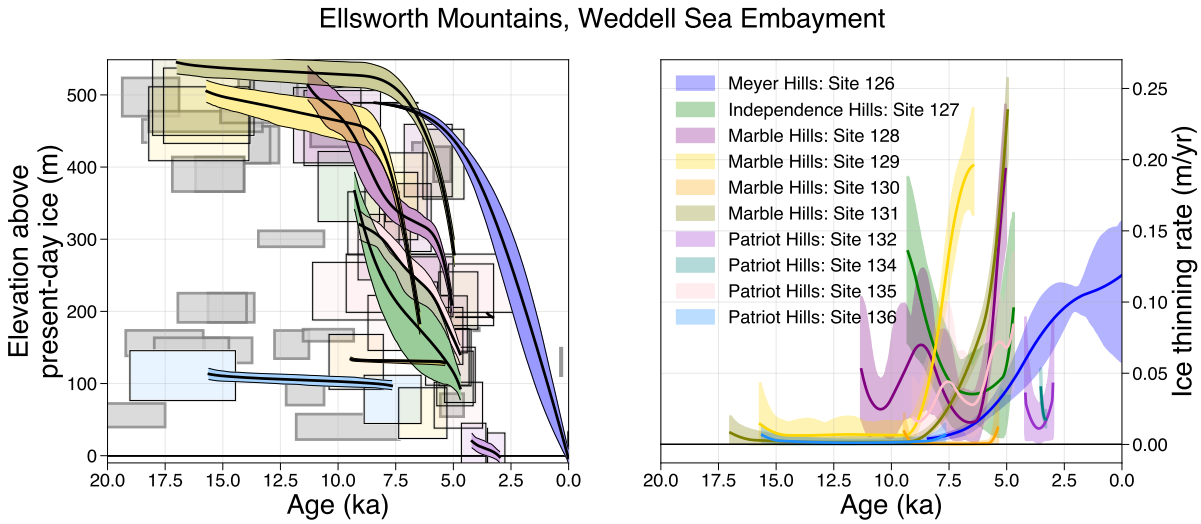

Fig. S61 Thinning histories from Ellsworth Mountains Weddell Sea Embayment. Colored boxes mark cosmogenic nuclide exposure age data and/or radiocarbon-dated lakes. Gray boxes mark rejected data. Colored envelopes denote PATR median and 95% credible intervals for local Antarctic Ice Sheet elevation (left panel) and rate of thinning (right panel).

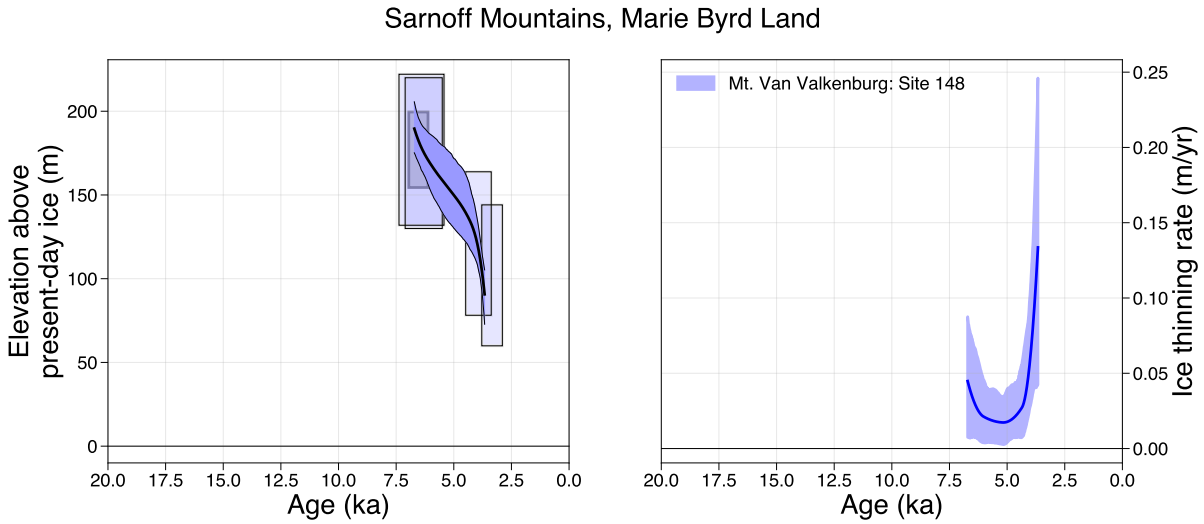

Fig. S62 Thinning histories from Sarnoff Mountains Marie Byrd Land. Colored boxes mark cosmogenic nuclide exposure age data and/or radiocarbon-dated lakes. Gray boxes mark rejected data. Colored envelopes denote PATR median and 95% credible intervals for local Antarctic Ice Sheet elevation (left panel) and rate of thinning (right panel).

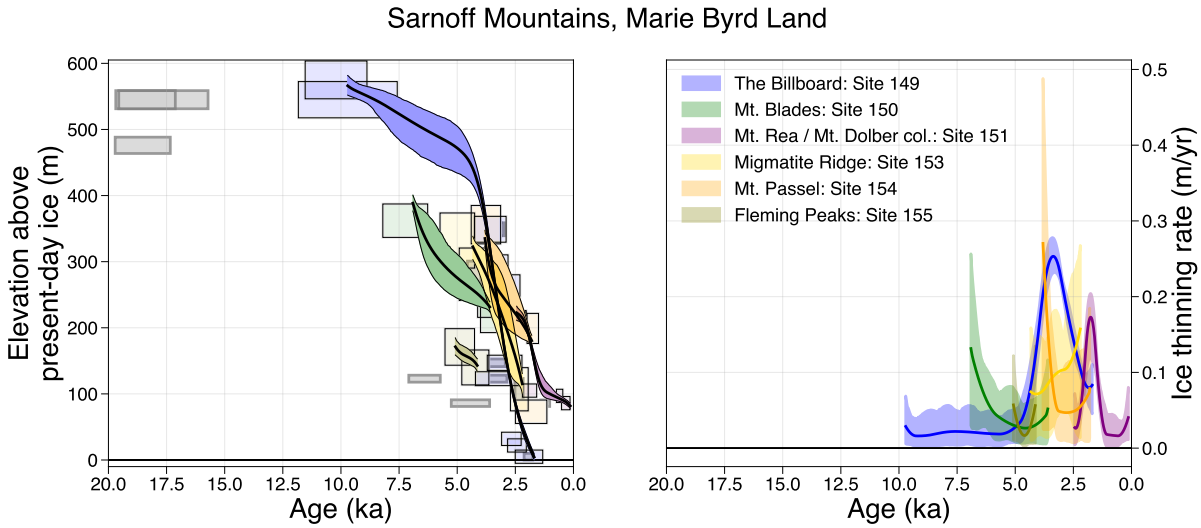

Fig. S63 Thinning histories from Sarnoff Mountains Marie Byrd Land. Colored boxes mark cosmogenic nuclide exposure age data and/or radiocarbon-dated lakes. Gray boxes mark rejected data. Colored envelopes denote PATR median and 95% credible intervals for local Antarctic Ice Sheet elevation (left panel) and rate of thinning (right panel).

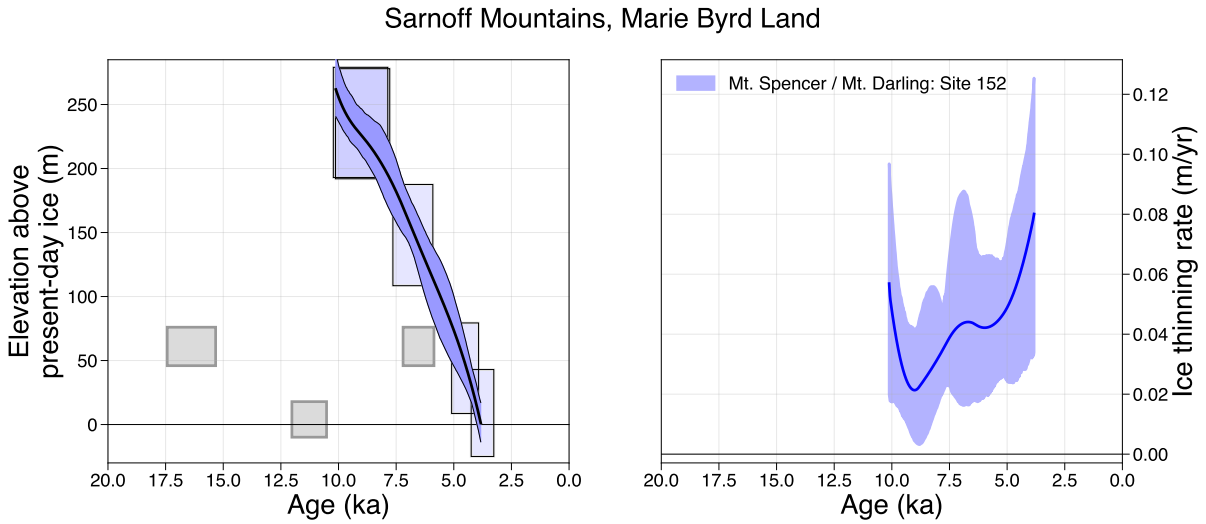

Fig. S64 Thinning histories from Sarnoff Mountains Marie Byrd Land. Colored boxes mark cosmogenic nuclide exposure age data and/or radiocarbon-dated lakes. Gray boxes mark rejected data. Colored envelopes denote PATR median and 95% credible intervals for local Antarctic Ice Sheet elevation (left panel) and rate of thinning (right panel).

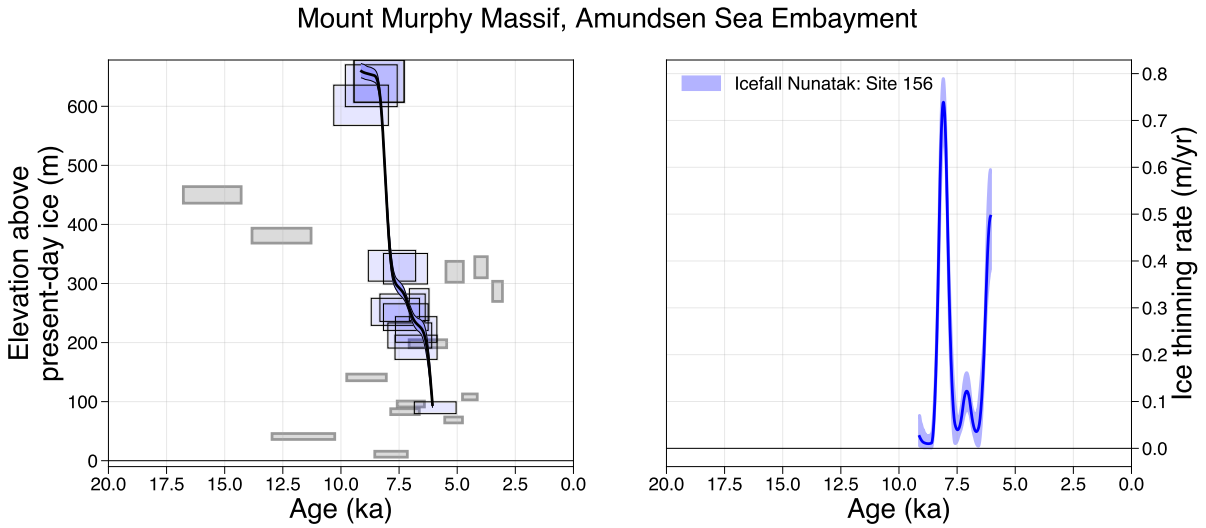

Fig. S65 Thinning histories from Mount Murphy Massif Amundsen Sea Embayment. Colored boxes mark cosmogenic nuclide exposure age data and/or radiocarbon-dated lakes. Gray boxes mark rejected data. Colored envelopes denote PATR median and 95% credible intervals for local Antarctic Ice Sheet elevation (left panel) and rate of thinning (right panel).

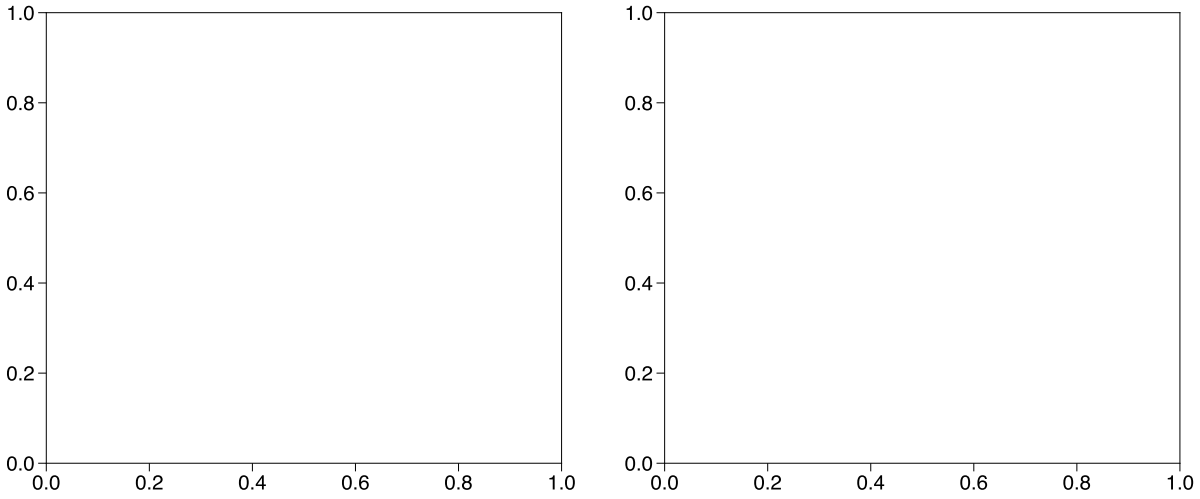

Fig. S66 Thinning histories from Bear Peninsula Amundsen Sea Embayment. Colored boxes mark cosmogenic nuclide exposure age data and/or radiocarbon-dated lakes. Gray boxes mark rejected data. Colored envelopes denote PATR median and 95% credible intervals for local Antarctic Ice Sheet elevation (left panel) and rate of thinning (right panel).

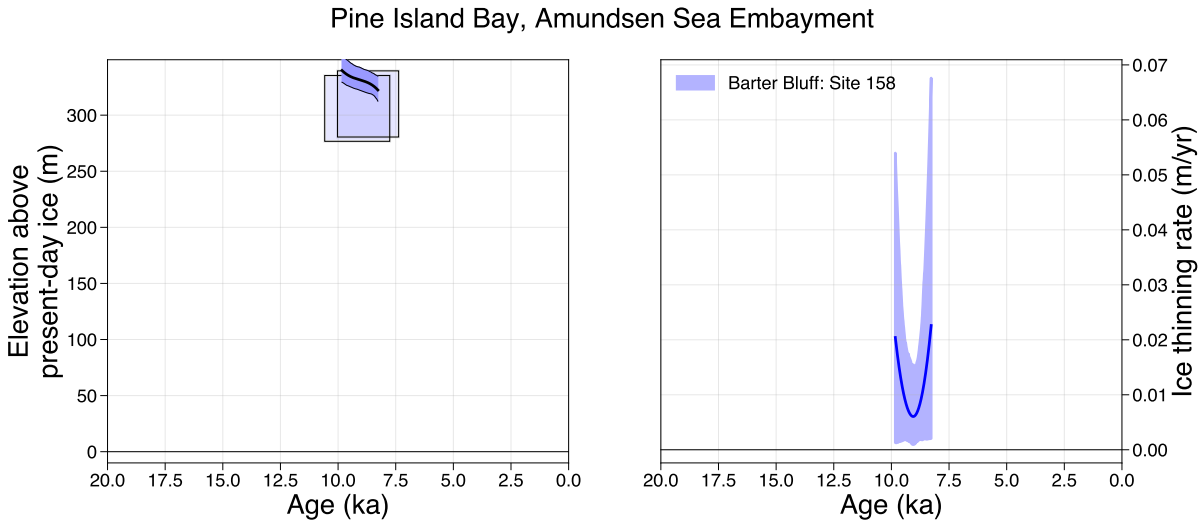

Fig. S67 Thinning histories from Pine Island Bay Amundsen Sea Embayment. Colored boxes mark cosmogenic nuclide exposure age data and/or radiocarbon-dated lakes. Gray boxes mark rejected data. Colored envelopes denote PATR median and 95% credible intervals for local Antarctic Ice Sheet elevation (left panel) and rate of thinning (right panel).

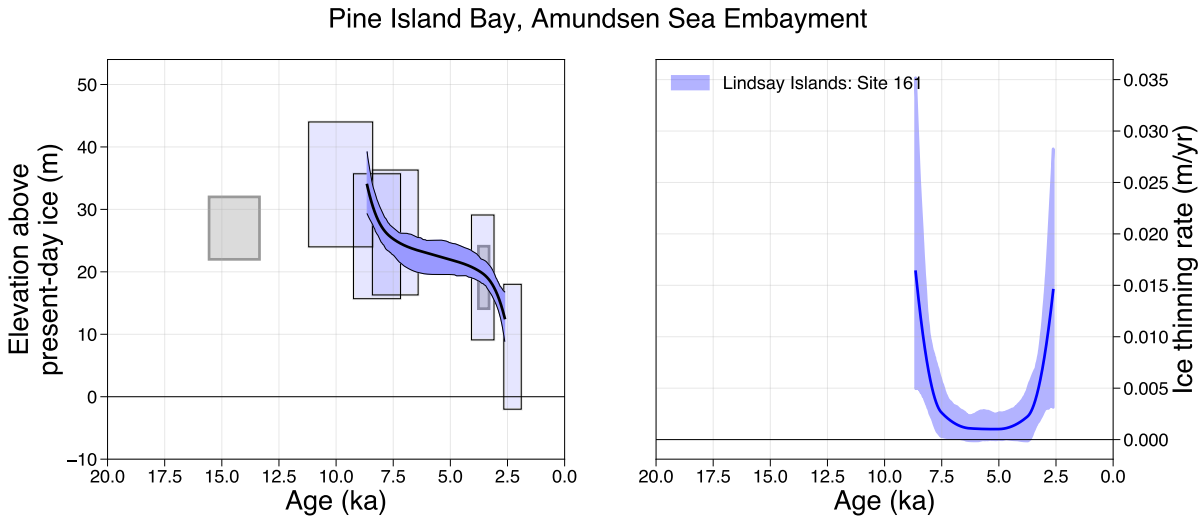

Fig. S68 Thinning histories from Pine Island Bay Amundsen Sea Embayment. Colored boxes mark cosmogenic nuclide exposure age data and/or radiocarbon-dated lakes. Gray boxes mark rejected data. Colored envelopes denote PATR median and 95% credible intervals for local Antarctic Ice Sheet elevation (left panel) and rate of thinning (right panel).

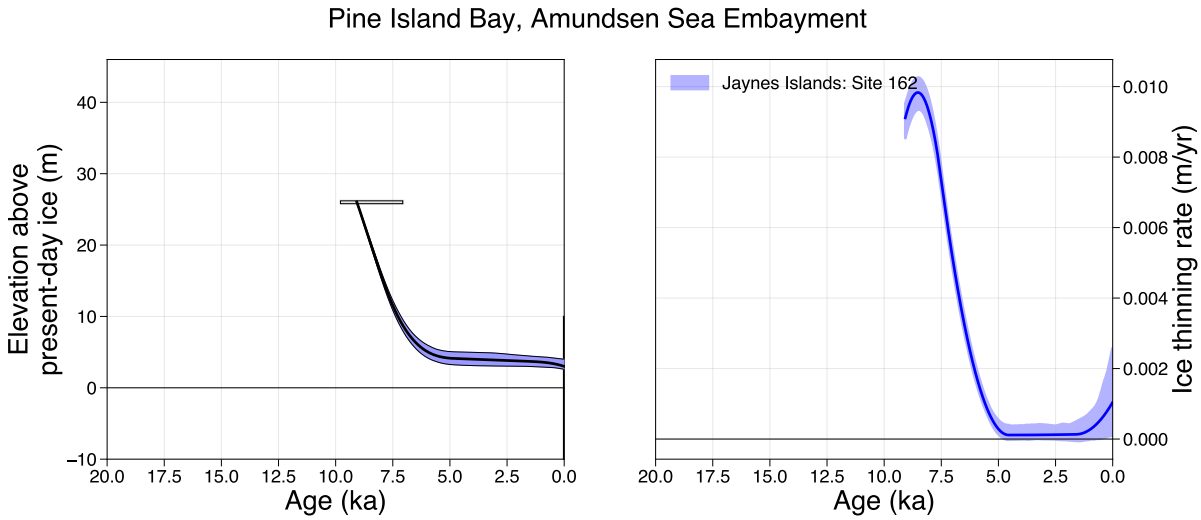

Fig. S69 Thinning histories from Pine Island Bay Amundsen Sea Embayment. Colored boxes mark cosmogenic nuclide exposure age data and/or radiocarbon-dated lakes. Gray boxes mark rejected data. Colored envelopes denote PATR median and 95% credible intervals for local Antarctic Ice Sheet elevation (left panel) and rate of thinning (right panel).

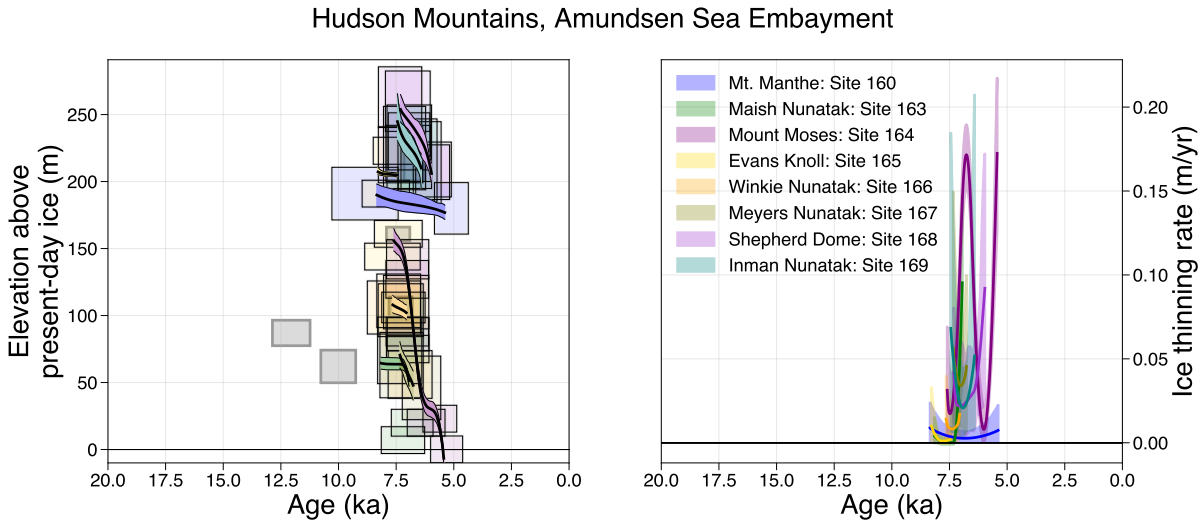

Fig. S70 Thinning histories from Hudson Mountains Amundsen Sea Embayment . Colored boxes mark cosmogenic nuclide exposure age data and/or radiocarbon-dated lakes. Gray boxes mark rejected data. Colored envelopes denote PATR median and 95% credible intervals for local Antarctic Ice Sheet elevation (left panel) and rate of thinning (right panel).

References

[1] Seroussi, H. *et al.* Evolution of the Antarctic Ice Sheet Over the Next Three Centuries From an ISMIP6 Model Ensemble. *Earth's Future* **12**, e2024EF004561 (2024). URL https://onlinelibrary.wiley.com/doi/abs/10.1029/2024EF004561. _eprint: https://agupubs.onlinelibrary.wiley.com/doi/pdf/10.1029/2024EF004561.

[2] Grieman, M. M. *et al.* Abrupt Holocene ice loss due to thinning and ungrounding in the Weddell Sea Embayment. *Nature Geoscience* **17**, 227–232 (2024). URL https://www.nature.com/articles/s41561-024-01375-8.